EXPERIMENTAL INVESTIGATION ON LASER MARKING OF LIGHT METAL AND ALLOY

A thesis submitted towards partial fulfilment of the requirements for the degree of

Master of Technology (M.TECH)

In

Laser Technology

A course affiliated to

Faculty of Engineering and Technology

And offered by

Faculty of Interdisciplinary Studies, Law and Management (FISLM)

Jadavpur University

188, Raja S. C. Mallick Road, Kolkata -700032

Prepared by,

SONA LAKHI YOLMO

Examination Roll No: M4LST22001

Registration No: 154556 of 2020-2021

Under the guidance of

DR. SOUREN MITRA

Professor, Production Engineering Department

Jadavpur University, Kolkata – 700032

School of Laser Science and Engineering
Jadavpur University
Kolkata- 700032
India
2022

M.TECH. IN LASER TECHNOLOGY
Course affiliated to
FACULTY OF ENGINEERING & TECHNOLOGY
Offered by
FACULTY OF INTERDISCIPLINARY STUDIES, LAW & MANAGEMENT
JADAVPUR UNIVERSITY

CERTIFICATE OF RECOMMENDATION

I, HEREBY, RECOMMEND THAT THE THESIS PREPARED UNDER MY SUPERVISION BY **SONA LAKHI YOLMO** ENTITLED **EXPERIMENTAL INVESTIGATION ON LASER MARKING OF LIGHT METAL AND ALLOY** BE ACCEPTED IN THE PARTIAL FULFILLMENT OF THE REQUIREMENTS FOR THE DEGREE OF MASTER OF TECHNOLOGY IN LASER TECHNOLOGY DURING THE ACADEMIC SESSION 2020- 2022.

THESIS SUPERVISOR
(Dr. Souren Mitra)
Professor, Production Engineering Department
Jadavpur University, Kolkata-700 032

Countersigned

DIRECTOR
(Sri Dipten Misra)
School of Laser Science and Engineering
Jadavpur University, Kolkata-700 032

DEAN
Faculty of Interdisciplinary Studies, Law and Management
Jadavpur University, Kolkata-700032

JADAVPUR UNIVERSITY

FACULTY OF INTERDISCIPLINARY STUDIES, LAW AND MANAGEMENT

CERTIFICATE OF APPROVAL **

This foregoing thesis is hereby approved as a creditable study of an engineering subject carried out and presented in a manner satisfactory to warrant its acceptance as a pre-requisite to the degree for which it has been submitted. It is understood that by this approval the undersigned do not necessarily endorse or approve any statement made, opinion expressed or conclusion drawn therein but approve the thesis only for the purpose for which it has been submitted.

COMMITTEE OF FINAL EXAMINATION
FOR EVALUATION OF THESIS

** Only in case the recommendation is concurred

DECLARATION OF ORIGINALITY AND COMPLIANCE OF ACADEMIC ETHICS

The author hereby declares that this thesis contains original research work by the undersigned candidate, as part of her **Master of Technology in Laser Technology** studies during academic session 2020-2022.

All information in this document has been obtained and presented in accordance with academic rules and ethical conduct.

The author also declares that as required by this rules and conduct, the author has fully cited and referred all material and results that are not original to this work.

NAME: **SONA LAKHI YOLMO**

EXAMINATION ROLL NUMBER: **M4LST22001**

REGISTRATION NUMBER: **154556 of 2020-2021**

THESIS TITLE: **EXPERIMENTAL INVESTIGATION ON LASER MARKING OF LIGHT METAL AND ALLOY**

SIGNATURE: DATE:

ACKNOWLEDGEMENT

I would like to express my deepest gratitude towards all those who have supported me in making this endeavour possible.

I could not have undertaken this journey without the support of my supervisor **Dr. Souren Mitra,** Professor, Department of Production Engineering, Jadavpur University. I am extremely grateful to him for his constant guidance and support throughout my work and for encouraging me in ways that made this possible. Not only has he inspired me in completing this research but also has always been so concerned about my career and pushes me to strive for better in life.

My sincere gratitude goes to **Sri. Dipten Misra**, Director, School of Laser Science and Engineering, for providing me the necessary infrastructure for carrying out experimental measurements and for all his support and concerns.

I would like to extend my deepest appreciation to **Ms. Upama Dey** for her valuable and constructive suggestions during the planning and development of this thesis work. She has been so generous in providing her valuable time every now and then and has guided me throughout with her enthusiastic encouragement and useful critiques necessary for completing my thesis.

I would like to extend my special thanks to **Mr. Mohit Pandey** for guiding me with all the experiment and metrological related matters where he has showered me with all the necessary knowledge about the machine details. Thanks to him for being so generous in providing me his valuable time and effort in making all the experiments possible.

I also had the pleasure of working with my batch-mates Sourav Das and Ajfarul Islam from Production Engineering Department, to whom I would like to acknowledge for being so welcoming in working together.

Last but not the least words cannot express my deepest gratitude to my lifelines, my dear parents, who has been a pillar support in whatever I do in life and for always having faith in me that makes everything possible.

My boundless gratitude goes to God and I would like to end her with a small quote from The Dalai Lama.

"A heart full of love and compassion is the main source of inner strength, willpower, happiness and mental tranquility."

SYNOPSIS

In the present research, Laser marking on Aluminium and Beryllium Copper has been performed to investigate the effect of some of the process parameters i.e. Power, Scanning speed and Frequency on the process responses i.e., Surface roughness (Ra) and Heat Affected Zone (HAZ). With the help of scatter plots, the relationship between the process parameters and the process responses has been analysed. Regression analysis is done to develop predictive model for the process responses and analysis of variance test (ANOVA) is done to check the efficacy of the model thus obtained. Finally using the mathematical model obtained from the fit regression analysis, optimization of the process parameters is performed using Multi-Objective Particle Swarm Optimization Technique (MOPSO). The objective of optimization taken is to maximize surface roughness and minimize heat affected zone. From the results thus obtained, the objective is fulfilled at a Power of 35W and Scanning speed of 8mm/s in case of Aluminium and for Beryllium Copper the values obtained are 15W and 4mm/s respectively for Power and Scanning speed. Pareto Front is constructed to show the quality of the final solutions thus obtained through the convergence and even distribution of the particles and also depicts the relationship between the two process responses i.e. surface roughness (Ra) and heat affected zone (HAZ).

TABLE OF CONTENTS

LIST OF TABLES

LIST OF FIGURES

CHAPTER -1

INTRODUCTION

1.1. Laser Micro-machining

Origin and Definition

Conventional Machining, the backbone of machining processes that has been existing since ages, is a process done by chip removal which is achieved by direct contact between the tool and the work-piece surface. With the recent advancements in the use of high strength material, environmental aspects and evolution of micro level products have given rise to a newer concept in material removal. As a consequence of this, non-traditional machining processes have emerged to overcome the loop holes caused by conventional machining. Amongst many such non-traditional machining technique, Laser beam machining is one such process which helps produce intricate shapes using lasers.

The world of laser machining is divided in micro and macro machining. The classification is made not on the basis of the size of the work-piece but rather on the fineness of impact caused by the laser. The laser system used for micro-machining generates very fine structures ranging in micro meters and generally uses pulsed beam with an average power well below 1 kW while those for macro-machining uses continuous wave with average power ranging up-to several kW. Laser micro-machining process requires rapid heating, melting and evaporation of materials to create intricate shapes and sizes. Lasers for micromachining offer a wide range of wavelength, pulse duration and repetition rates which allow micro-machining with high resolution in depth and lateral dimension. [1]

Some of the benefits of Laser micro-machining are as follows [2]:

i. It is a non-contact process. It does not require any external tool and hence there are no chance of mechanical damage by the tool to the parts being processed. Following this, there is no tool wear and hence it is cost effective as compared to other non- traditional processes like EDM.
ii. It can also be a one step process unlike for e.g. etching which requires toxic chemicals and is a multistep process. Also by simply varying the parameters like wavelength, pulse duration, energy density, etc., one can get selective material removal.

iii. It is a very flexible tool as it incorporates computer control and simply by changing the program one can perform different types of operation and obtain different features on the work-piece.

Applications

Some of the industrial applications of Laser Micro-machining areas follows [1].

a) Microelectronics and Semiconductors- Micro- drilling
b) Bio/Chemical Devices- Production of Microfluidic systems
c) Defence/Aerospace- Wire Stripping and Marking
d) Automobiles - Manufacturing of automotive fuel filters, which require small holes through up to 1 mm, laser drilling fuel injectors for gasoline and diesel, etc.

1.2. Light Metal and Alloy

Lightweight metals are those that have low density and high strength to weight ratio. They are also characterised by low toxicity unlike heavy metals. They hold increasing importance in the automotive manufacturing sectors, aircraft, heavy duty trucks, rail, ship, defence industries, etc. The metals that come under this category are aluminium, beryllium, titanium and magnesium and its alloys. They are needed in applications that require light weight with improved performance as in the case of aerospace, marine, medical applications, etc. There are many techniques available for processing light-weight metals such as melt processing, powder processing, thermo-mechanical processing, forming, coatings, and joining and assembly [3].

Aluminium

Origin of name: The name has been derived from the Latin word “alumen” meaning bitter salt also used to describe potash alum KAl(SO4)2·12H2O.

Description of the metal: Aluminium is the most abundant metal found on earth comprising 8.1% of the earth’s crust and one of the most widely used non-ferrous metal. It is never found in metallic state and is always present with other elements like oxygen, fluorine and silicon and in minerals like bauxite and cryolite. It is extracted from mineral Bauxite. The Bayer process is used to convert bauxite to aluminium oxide and using electrolytic cells and Hall Heroult process this is then converted to pure aluminium.

It appears as a silvery- white lightweight metal which is soft and malleable. It is normally mixed with other metals to form aluminium alloys which are harder and stronger.

It is also found in powder form and appears as a light grey solid which is denser than water and its contact may burn skin [4,9].

Fig.1.1. Aluminium sheet.

Properties of Aluminium:

Aluminium has thermal conductivity more than that of steel making it an important material for heating and cooling applications. It has an added advantage of being non-toxic making it idea for use as kitchenware and cooking utensils.

It has a very high reflectivity (about 80% reflectivity for visible light) which makes it ideal for use as an insulator to protect against sun's rays in summer and prevent heat loss in winter [9,5].

Table 1.1.below shows some the basic properties of aluminium.

Table 1.1. Properties of Aluminium

Group	13
Period	3
Block	p
Atomic number	13
State at 20°C	solid
Melting point	660.323°C, 1220.581°F, 933.473 K
Boiling point	2519°C, 4566°F, 2792 K
Density(g/cm^2)	2.70
Relative atomic mass	26.982
Specific heat capacity (J kg−1 K−1)	897
Shear modulus(Gpa)	26.1
Young's modulus(Gpa)	70.3
Bulk modulus(Gpa)	75.5

Uses of Aluminium

a) The properties of aluminium like low- density, non-toxic, high thermal conductivity, excellent corrosion resistance and easily machinable, cast and formed has made it available to be used in number of products like kitchen utensils, cans, foils, window frames, aeroplane parts, etc.
b) Pure aluminium not being so strong in itself is alloyed with copper, magnesium, manganese and silicon resulting in a stronger and harder material though they are lightweight. This holds an extremely important application in the construction of aeroplanes and other forms of transport.
c) Its good electrical conductivity makes its use in electrical transmission lines. It is also reasonable than copper.
d) When aluminium is evaporated in vacuum, it forms a highly reflective (heat and light), non- deteriorating coating which has a great application for use in telescope mirrors, toys, decorative packages(foils), etc [9,5].

Beryllium Copper

Description of the metal alloy: Beryllium alloy, also known as copper beryllium, spring copper and beryllium bronze, is one of the highest strength alloy of copper in which the content of beryllium is 0.3%-2.0% and along with it other elements can also be present. It is made by combining beryllium, a low density metal with a steel grey colour, with copper and other elements. It is non-ferrous and known for high strength, non-magnetic and non-sparking qualities which makes it ideal to be used in hazardous environments. Depending on the concentration of beryllium present, there are wide range of grades available and is classified into high strength alloys and high conductive alloys accordingly [6].

Fig. 1.2. Beryllium Copper sheet.

Properties of Beryllium Copper

High electrical and thermal conductivity

a) Non- sparkling and non-magnetic
b) High ductility and excellent formability and hence has excellent metalworking, forming and machining qualities.
c) Highly corrosion and oxidation resistant than steel
d) High durability than most copper alloys, wear and galling resistant.
e) Can retain its properties in extreme environmental conditions.
f) High fatigue strength making it suitable for heavy cyclic load applications.

Uses of Beryllium Copper:

a) Its non-sparkling properties makes it suitable to be used in hazardous environments like oil and gas industries as oil rig component and mining tools.

b) Its ability to retain its shape even under repeated stress and strain makes it ideal to be used in springs, spring wire, load cells , bushings for aircraft undercarriages, drums and rollers in ball bearings, and tools in the oil and gas industry for deep-hole drilling, which require the outstanding properties of CuBe to withstand cyclical loads.

c) Its high thermal conductivity makes it to be used in low- current contacts for batteries and electrical connectors.

d) It is also used as MWD (Measurement while drilling) tools since non-magnetic alloys are required.

e) Hence this alloy finds huge applications in computer and electronics industries, telecommunications, musical instruments, injection mold design, etc. for its huge qualities [6].

1.3. Laser Marking

Definition and its applications.

What is Laser marking?

Laser marking is a modern process of creating a permanent mark on a surface by using a beam of concentrated light generated from a laser source. The beam of light upon interaction with the material changes the appearance of the surface creating a certain design. This process can be performed using various types of laser sources, to name a few are fiber, pulsed, continuous wave, UV or green lasers, etc. This process can be performed on a wide range of materials viz. metals, non-metals, ceramics, plastics, glass, polymers, etc. and encompasses a wide variety of applications.

It contributes to a wide percentage of laser related applications among others.

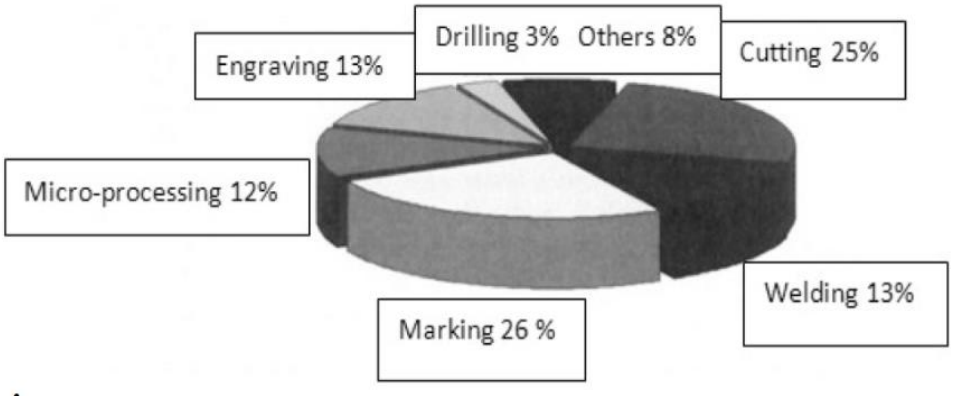

Fig 1.3. Percentage of laser used technologies.

This latest technology holds application in many industries like electronics, automobile, mechanical engineering, medical industry, etc. Like mentioned earlier, it has a wide range of applications and depending on that there are various types of laser marking methods. They are as follows [10]:

1. Laser engraving- here the laser removes the part of the parent material and a depression is created. Depth is created in this type of laser marking.

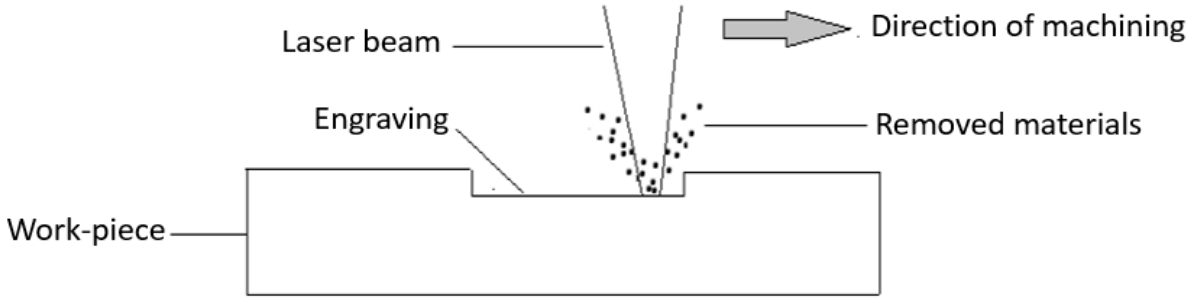

Fig 1.4 Laser engraving

2. Ablation- here the material gets removed in layers usually by melting and/or vaporization.

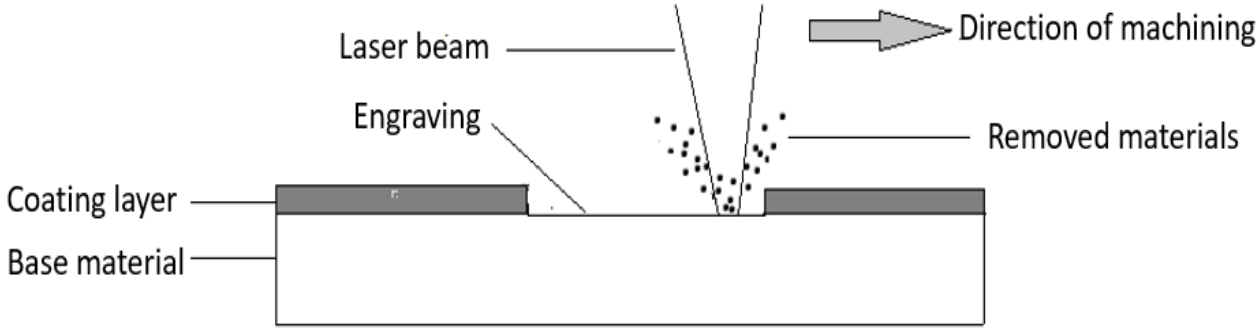

Fig 1.5. Ablation

3. Annealing/colour change- here the laser heats the surface altering the colour. The surface remains smooth.

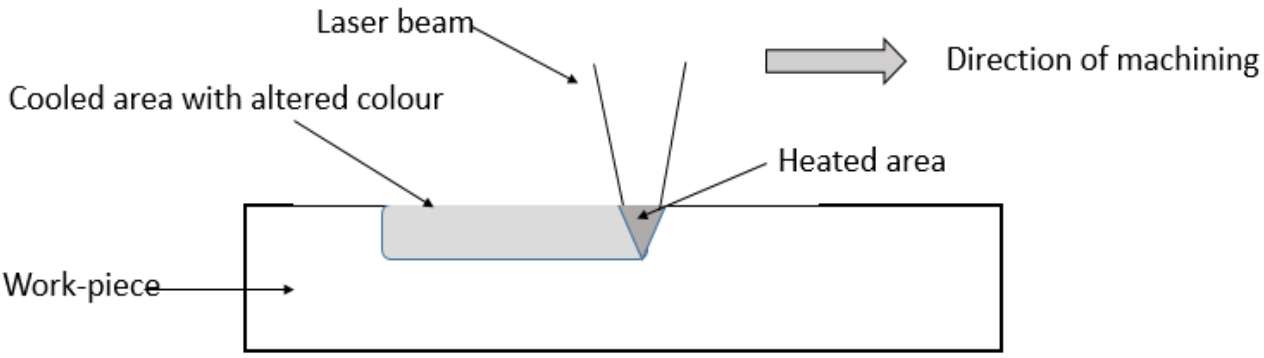

Fig 1.6. Annealing/colour change

4. Foaming- this is normally done for marking on plastics where the interaction between the laser and the material leads to the formation of a gas bubble which causes the appearance of a raised or textured mark.

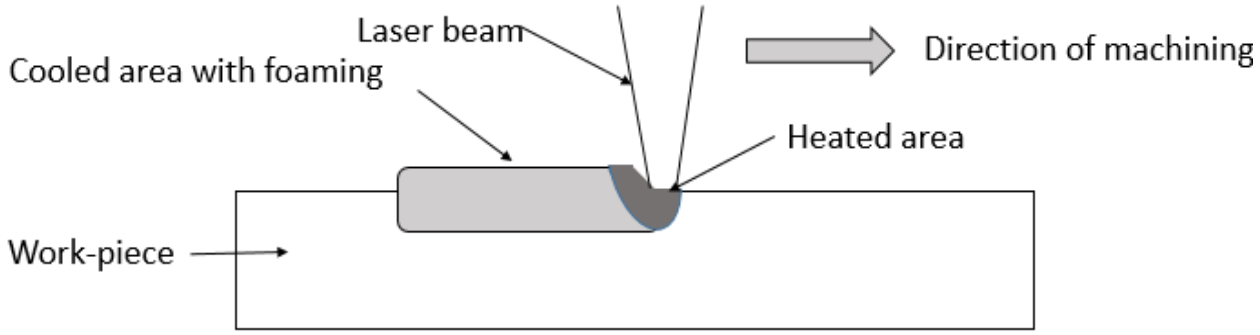

Fig 1.7. Foaming

Some of the traditional marking technologies

Before Laser Marking, some of the traditional marking technologies available are as follows:

a) Ink jet marking- a technique which marks by forcing ink through the nozzles on the material. Material has to be moving always.
b) Dot peening – here a pneumatically driven stylus is available which marks on an object through indentation.

c) Electrochemical etching- an electrolytic solution, an electrode marking head and a pre-produced mask is required which does the marking through forced corrosion producing a black oxide layer on the surface where the image is engraved.

These marking technologies require additional resources like toxic consumables, need for a stylus and a pre-produced mask respectively in order to do the marking. Some of them are contact marking techniques which has to bear an additional tooling cost. The use of toxic chemical in case of ink jet marking is harmful for the environment. In this way there are other cons that make these technique not so advisable for marking on materials.

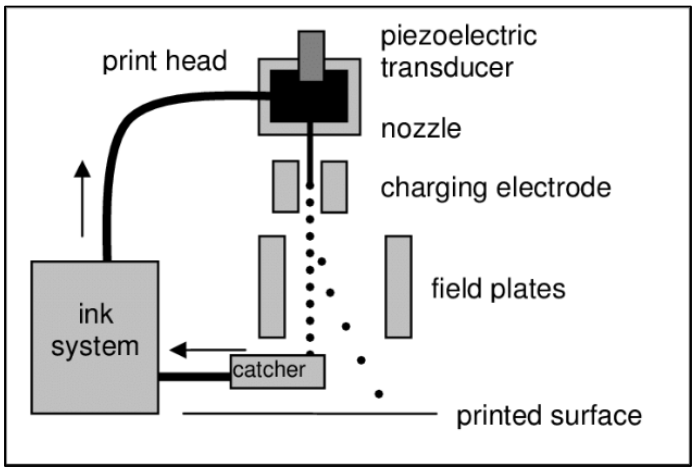

a)

b)

Fig. 1.8. Traditional marking technologies. a) Ink-jet marking; b) Dot peen marking

1.3.1. Need for Laser marking

Laser marking contains a huge number of benefits because of which a number of industries need Laser marking in its production line. The following are some of the benefits that explains why Laser marking is needed [7].

i. It allows the modern day producers to identify and track their products throughout the supply chain for quality control, inventory management, monitoring production, etc., ultimately facilitating them in process improvement. For this purpose marking automated information on the product like serial numbers, barcodes, QR codes, or logos, alpha numerals, etc., are the key to achieve this objective which is fulfilled by Laser marking.
ii. It can be easily integrated with the production line and facilitate automation. Once the part is identified at the beginning of the production line, barcode scanners can be employed at each step of the production which allows the producers to trace and track every product and for quality improvement, it allows to store important information of the product on the database.
iii. It is a contactless, low maintenance technology, has no moving parts and doesn't use any kind of consumables or additional tools like ink jet printing, dot peening methods to create a mark which means that operators are not needed to operate the marking manually and rarely needs to maintain it.
iv. It is highly economical as it is extremely fast, contactless hence no tool wear, can mark extremely small features with great precision, doesn't require any toxic consumables hence highly environment friendly.

Some of the special characteristics of Laser marking are as follows.

i. As mentioned earlier, it is a non- contact process hence it allows marking on both hard and ultra-hard materials for mechanical engineering and brittle and thin materials for micro- electronics industries.
ii. It has the ability to interact with the material selectively and undergo heating/melting/evaporation on a very small area giving it a benefit over other marking technologies.
iii. The modern laser scanners has the ability to control the movement of the beam and position it with great precision which has also contributed to the entry of this technology in modern day production of various products.

The main industries that need marking solutions are the automotive, primary metals (including aluminium, steel, zinc, lead, and copper), extrusion, manufacturing, and converting industries.

1.3.2. Scheme of Laser marking

For Laser marking to take place, following are some of the basic components that are needed in a Laser marking system [8]. They are:

a) Laser source generator
b) Controller
c) Beam delivery system (galvanometer scan head/ mirrors, focussing lens, etc.)
d) X-Y table

The process of laser marking starts by generating a beam of laser radiation from **a laser source**. To generate a laser beam that can mark the surface of a material, light is amplified by stimulating photons. This is done by charging a material which release electrons and this charged electrons release its energy in the form of light (photons). As photons naturally stimulate the material's atoms, its electrons release more and more photons. This creates a concentrated ray of light called the laser beam.

The controller controls the direction, speed, pattern of marking and the intensity with which to mark the material. It contains necessary software that contains programs regarding the kind of data to be marked. It executes the program once the signal is received.

This beam of concentrated radiation travel through the **galvanometer scan head** which contains mirrors such that it directs the laser beam in direction according to the kind of mark that is required. This helps in creating a high contrast high quality marks.

This concentrated light then travels through the **focussing lens** which focuses the laser spot onto the work-piece. By using different laser marking process it is possible to create marks on the surface, deep into the material or under the surface.

Usually the work-piece is stationary and the laser moves in two dimensions drawing the pattern or both are stationary and galvanometer mirrors move the beam over the work-piece.

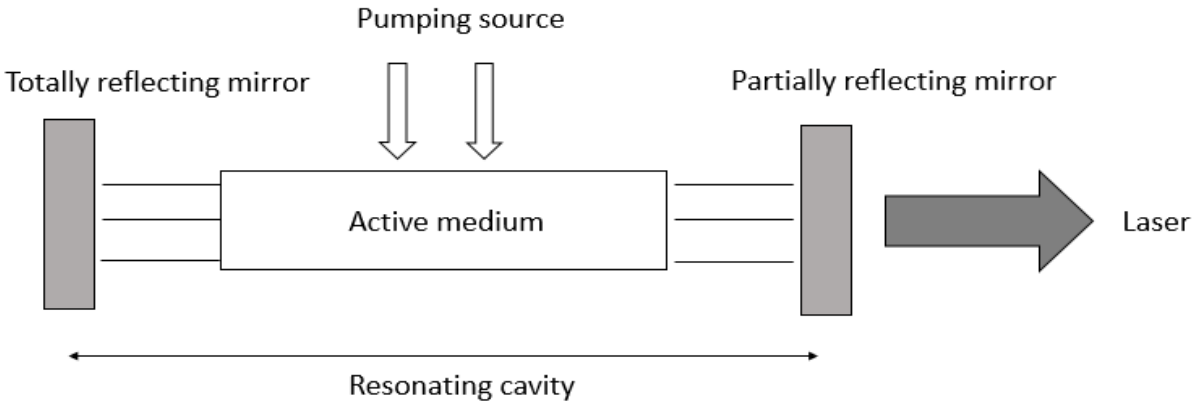

Fig. 1.9. Laser generation process

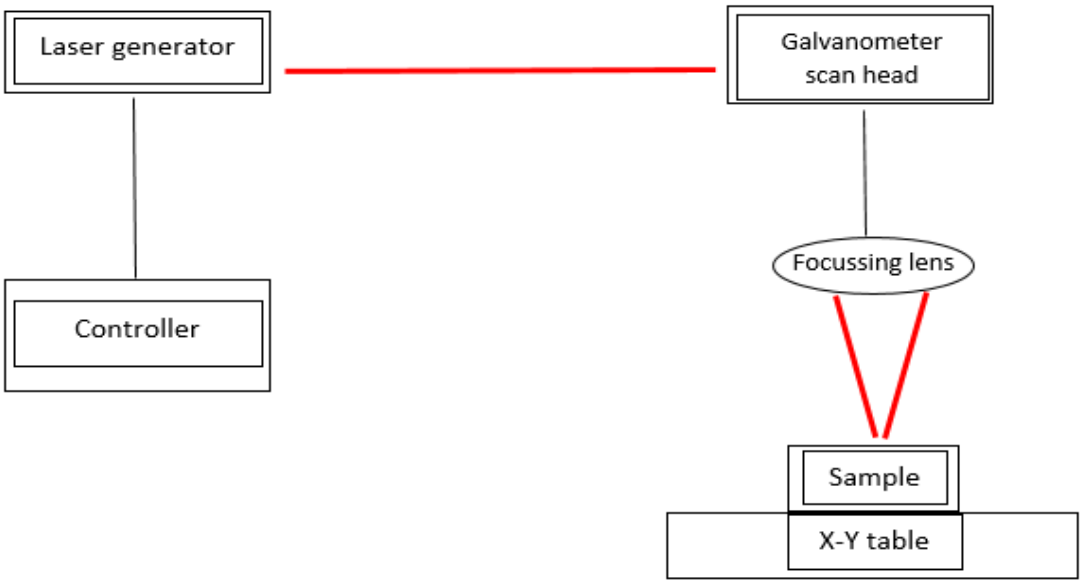

Fig. 1.10. Laser marking set-up

1.3.3. Physics of Laser marking

1.3.3.1. Working principle

Laser marking is the result of the impact caused by the beam of concentrated radiation coming from a laser source. During the interaction, the electromagnetic radiation of the laser beam is converted to thermal energy as shown in Fig 1.11. It is important to know the amount of energy that is absorbed by the material and its impact on it. During the process losses due to scattering, reflection, heat conduction, convection and thermal conductivity takes place and hence only that part of absorbed energy makes a real contribution towards the structural changes i.e., melting, vaporization or colour changes of the material [11].

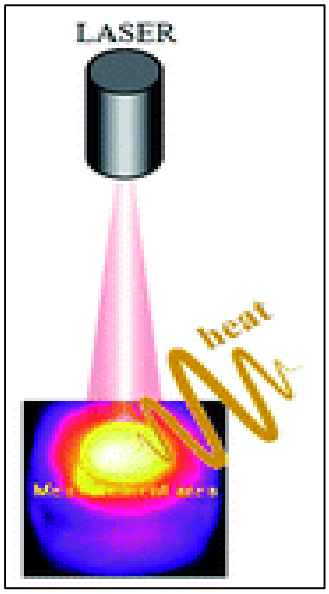

Fig.1.11 Conversion of electromagnetic radiation to heat.

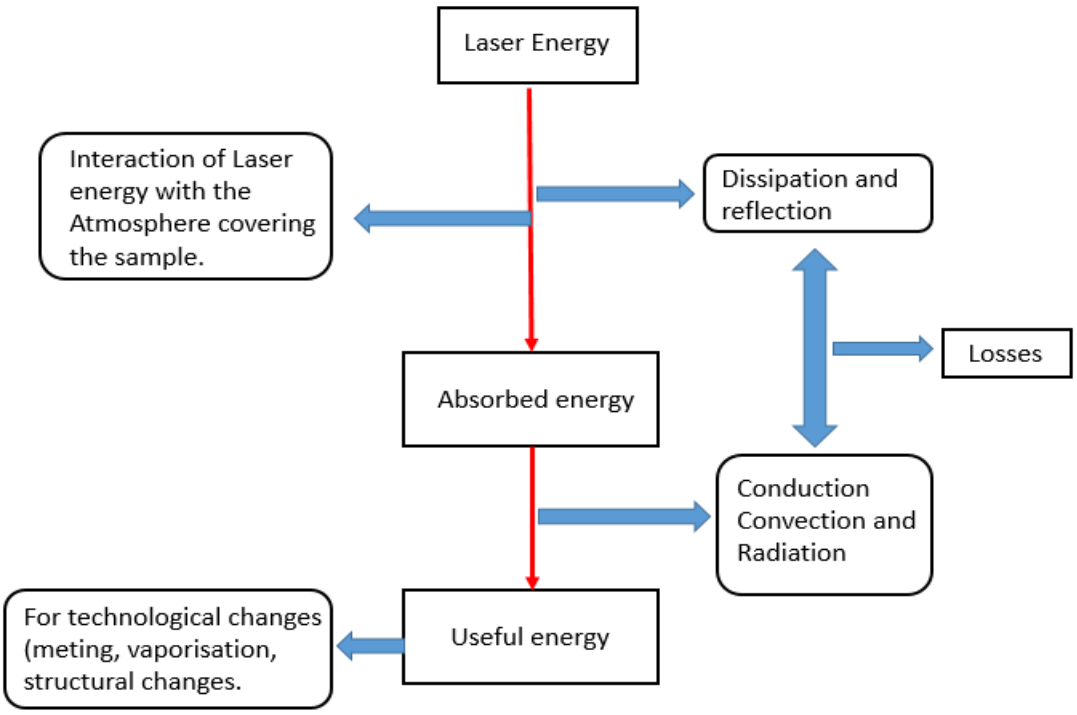

Fig. 1.12. Energy balance flow diagram of Laser impact on metals/alloys.

The absorption coefficient of the material plays a major role in the interaction of the laser radiation with the material. According to the previous research conducted, this absorption coefficient depends on the material properties like coefficient of reflection, surface topography (roughness), presence of oxides, nitrides, graphite layers, and physical properties of laser like

wavelength, power density, etc. The graph shown below shows the dependence of absorption on the wavelength of the laser.

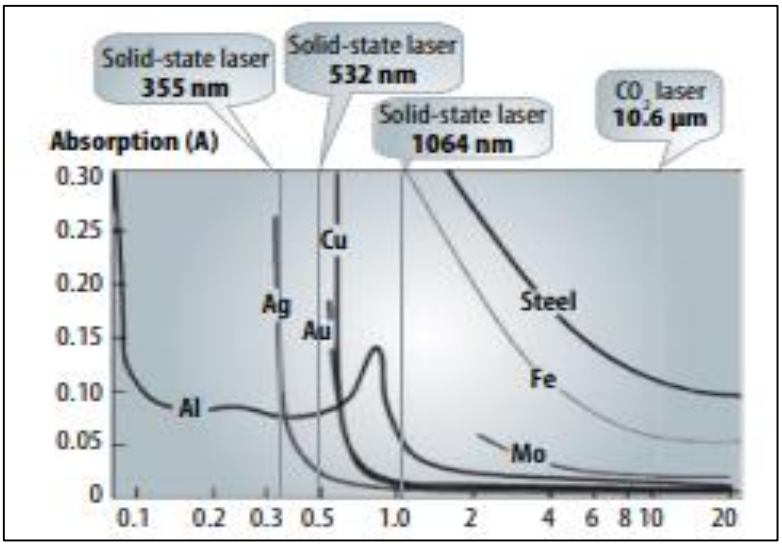

Fig. 1.13. Absorptivity vs. wavelength of different metals for selected lasers (reflective materials are silver (Ag); gold (Au); pure copper (Cu) and aluminium alloys (Al).

It is clear from the graph that as the wavelength increases absorption decreases for all kinds of materials. Ferrous and non-ferrous materials have excellent absorption at 1064 nm, while precious metals do so at 355 and 532 nm.

Another important factor that affects this absorption is the temperature of the laser impact surface. Fig 1.14.below shows how absorption changes for different temperature for the same material (in this case Al).

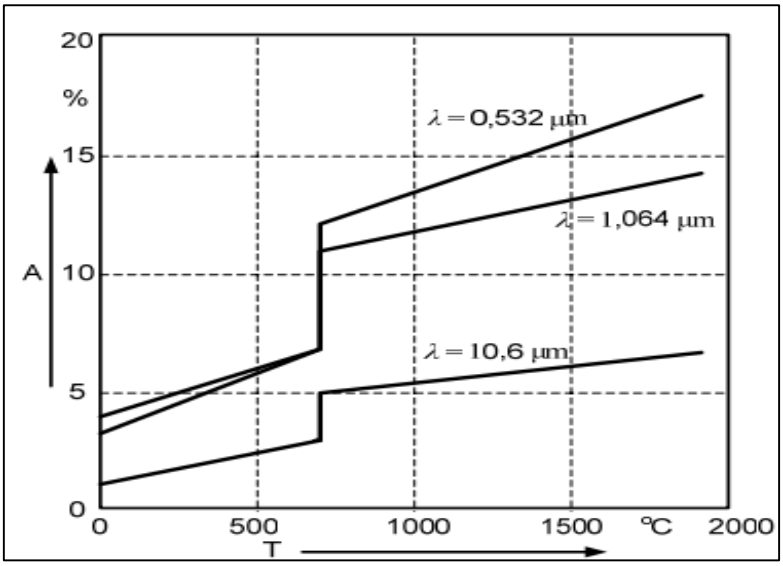

Fig.1.14. Dependence of absorption w.r.t temperature for different wavelength.

The main part of transmission of heat occurring during laser interaction is due to electron conductivity which is similar to the heat impact caused by traditional heat sources. Hence the theory of heat propagation can be explained using the thermal conductivity theory which is defined by the following differential equation [12].

$$\varsigma\rho\frac{\partial T}{\partial t} = \nabla.(\kappa\nabla T) + \alpha Q \qquad \text{Eq. (1.1)}$$

Where, T is temperature; ς- specific heat capacity; ρ – density of material; κ – coefficient of heat conductivity; Q – surface power density of laser radiation: α – coefficient of absorption.

With the help of this equation many theoretical research based on for e.g. Temperature distribution, calculation of critical pulse energy for melting/vaporization, etc., can be done.

Once the laser radiation is penetrated into a metal, it is completely absorbed by free electrons up-to a depth of about 0.1-1um which is the reason for the increase of energy taking place. This energy is also transferred to the crystal lattice from the beginning of the impact which leads to strong overheating of the electronic gas (Te>>Tl, Te=temperature of electronic gas, Tl= temperature of crystal lattice). After certain time, the state in the working volume has a property of shared temperature of the metal.

1.3.3.2. <u>Material removal mechanism</u>

Material removal during laser marking takes place with the help of ablation technique. Ablation means the removal of material either thermally or using photochemical erosion.

<u>Thermal ablation</u>- During thermal ablation, the excitation energy rapidly converts into heat, resulting in temperature rise and this can result in the ablation of material by surface vaporization or spallation (melt expulsion) which is caused due to thermal stresses. A thermal ablation mechanism is much more useful for the material removal during micromachining of both metals and ceramics.

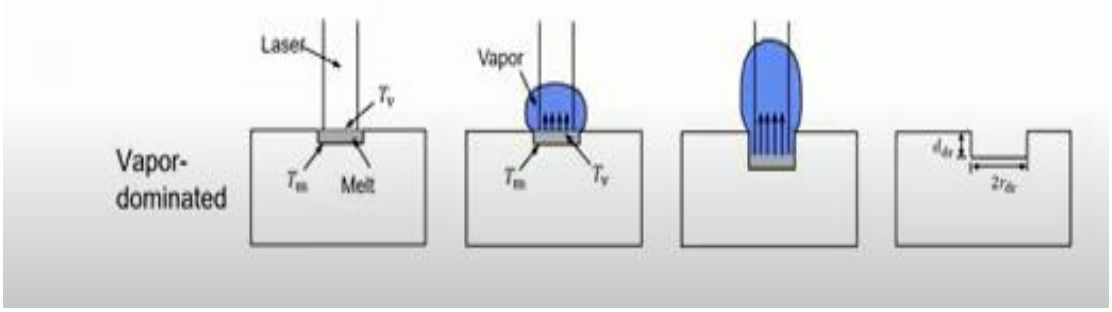

a)

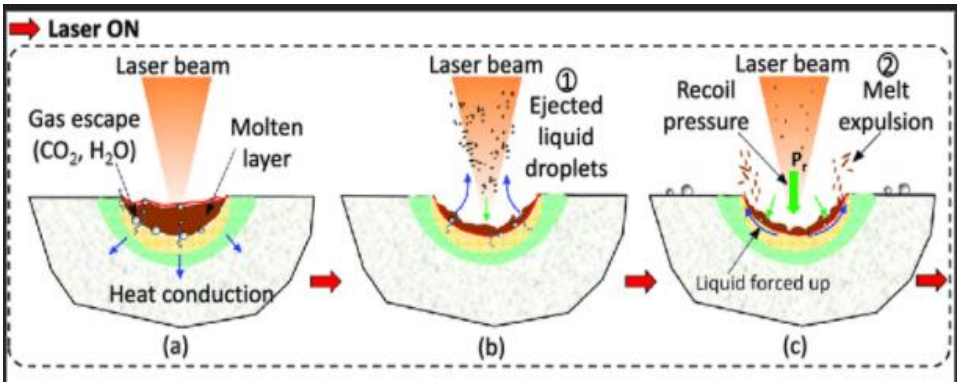

b)

Fig. 1.15. Thermal ablation a) Vapour dominated ablation; b) Material removal mechanism by spallation.

Photo chemical/non-thermal ablation- In this process, the energy coming out from the incident photon results in the direct breaking of the bond of the molecular chains in the organic material with the help of molecular fragmentation without any thermal damage.

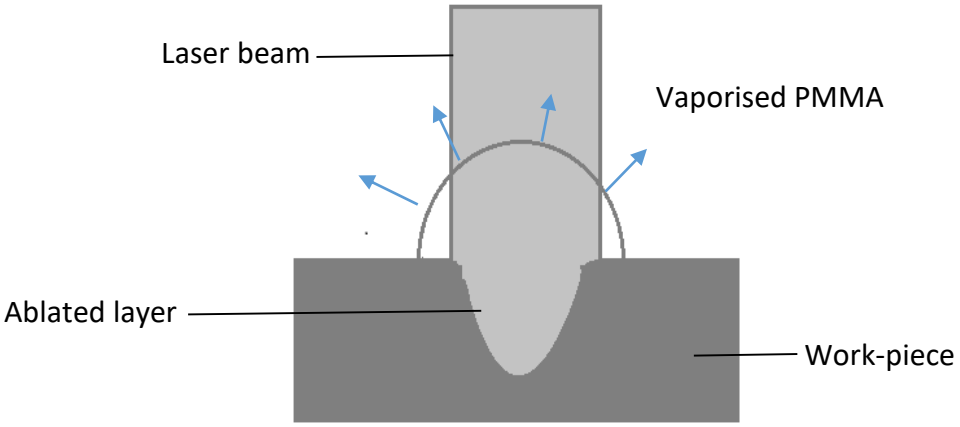

Fig. 1.16. Laser ablation of polymer (PMMA) by combination of photochemical and photo-thermal process.

1.3.3.3. *Parameters involved in Laser marking*

Parameters that affect Laser marking can be classified into two categories [10]:

i. Laser parameters
ii. Material properties

Laser parameters

Critical laser parameters that affect Laser marking are as follows.

- Power- It is the amount of optical power that the laser outputs. It is expressed as a percentage of the power level of the laser.
- Frequency- It is the number of pulses emitted by a laser in 1 sec. It is measured in terms of hertz. It has an inverse relationship with pulse energy
- Scanning speed- It is the distance travelled by the beam while marking the object .It is expressed in mm/s. Using a slow speed will create a deep and well defined mark while using a very high speed will have no effect on the material.
- Pulse duration- In simple words it is the time period for which the laser action is on. It is defined as the full width at half maximum of laser's optical power v/s time. Shorter the pulse duration, better is the quality of the mark as in case of ultra-short pulses.
- Fill spacing- It is the distance between the fill lines. Smaller fill lines leads to denser marks increasing the cycle time. Large fill spacing will create gaps in between the lines that is used to fill the characters. It is measured in mm
- Fill angle- It is the angle at which the laser beam moves while filling the characters.
- Number of passes- It represents the number of times the laser passes over the object. The more the pass, the deeper is the mark and the longer the time.

Material properties

Given below properties of the material play a key role in influencing the kind of laser marking technology to be used and the quality of marking obtained.

- Absorptivity and Reflectivity- The absorptivity is the most important material parameter of the work-piece in laser-material interaction. It is dependent on the combined parameters of the laser like wavelength, angle of incidence, laser radiation polarization as well as the materials radiative property, state, geometry of the surface and the temperature. As can be seen in the Fig. 1.13. above which shows the dependence of absorptivity with respect to the wavelength, for ferrous and non-ferrous material have great absorptivity at 1064nm wavelength while precious metal do so at lower wavelengths of 355nm and 532nm. The high initial reflectivity of materials like Ag, Au, Cu and Al alloys, can be overcome as long as the intensity of the laser beam is sufficiently high. The absorption rate increases remarkably as the temperature of the

material rises. Hence to initiate laser cutting or welding, metals with high surface reflectivity require higher intensities compared to materials such as steel.

- Thermal properties- Properties like thermal conductivity, heat capacity, melting point, vaporizing point etc., of the material affects the laser application on a material.

1.3.4. Types of Laser markers and their applications

1. *Fiber Lasers*

These laser marking machines are the ones most in demand after the invention of direct part marking. Their power ranges from 20-50W. They have an advantage of producing a small beam diameter with high quality, making it applicable for small component batch marking applications.

Application- They are useful for depth engraving or where one needs high power with small spot size to achieve high resolution. Some of the applications of a fiber laser are as follows.

I. Colour marking- This is a form of marking wherein the material is heated to change the colour of the surface resulting in different shades or where the coating layer is removed displaying the underlying material. This is useful for marking on packaging materials, fitting, labels, etc.
II. Annealing- This is a process of hardening the material using laser as a heat source in which case colour changes can also appear.
III. Foaming- The kind of marking that leaves the targeted area lighter than the rest part. It is mostly used in plastics wherein the heating results in formation of gas bubbles giving the mark a raised appearance.
IV. Carbonizing- It is a form of marking normally used for metals and metal alloys in which carbon molecules are destructed and made to bond with the metal itself bringing the carbon properties to the surface resulting in a darker/black mark.
V. Night and day marking – This marking is required for applications like reflectors, number plates, dashboards, etc., wherein the mark can be easily legible during the day and illuminated at night.

2. *Green Lasers*

These lasers appear in the Near-infrared region of the electromagnetic spectrum emitting at a wavelength of 532nm with power ranging between 5-10W. They have an advantage of greater absorption in a wide range of materials due to its low wavelength making it possible to mark on materials which cannot be marked using other high wavelength lasers. They can also give very less spot sizes of up-to 10um.

Applications-

They are useful for marking highly reflective materials with good precision. Materials like soft plastics, PCB boards, Integrated Circuit chips, etc., can be marked with good quality using this laser.

3. *UV Lasers.*

These lasers are those whose wavelength ranges between 10-400 nm in the electromagnetic spectrum. UV lasers are ideal for marking on organic molecules as the property of UV light is such that chemical and biological effects prevail more than simple heating. Other types of lasers like gas lasers, solid state lasers, diode lasers, etc., can be used to make a UV laser marking machine. This machine is ideal for applications that does not require heat generation like "cold marking".

Applications:

a) Used for marking on low heat tolerant materials like plastics, ceramics and can mark on glass without the need of additives and without causing micro-fracture.
b) They have high beam quality hence ideal for performing micro-marks on electronics, circuit boards, micro-chips

4. *CO2 Lasers*

These lasers emit at a wavelength of 10600nm and represent one of the oldest marking machines that are ideal for marking on non-metal surfaces like wood, ceramics, quartz, etc. For marking on metals, the metal has to be pre-treated using a special marking agent normally a spray to create a permanent mark.

Applications:

a) Good for marking, plastics on non- metallic surfaces like wood, ceramic, etc.
b) Suitable for glass marking.

5. MOPA Lasers

These lasers are a newly developed lasers which is similar in design to fiber lasers however have a different technology used. They use a Master Oscillator that helps in increasing the power of the beam without changing its properties. Hence this laser is said to have a high power efficiency because of the use of the master oscillator. It has the capability of adjusting the pulse width thereby giving different marking results which makes it capable of marking plastics.

Applications

a) They are suitable for doing reproducible multiple colour marking on stainless steel, black marking on anodized aluminium and high contrast marking on plastics.
b) The multiple colour marking is required by handcraft manufactures and hence this laser helps obtain designs of different colour on the material like stainless steel.

Brief discussion on how UV and IR lasers affect material processing

As we can see that the lasers above either emit rays in UV region or the near –IR or IR region of the electromagnetic spectrum. The electromagnetic spectrum shown in Figure 1.17 below shows some available laser wavelength [1].

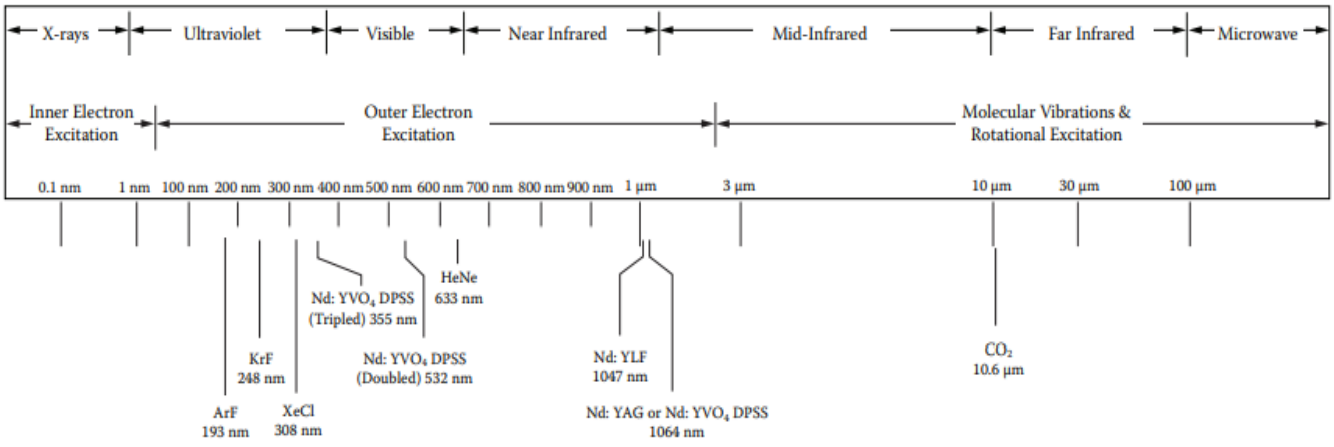

Fig. 1.17. The electromagnetic spectrum showing some available laser wavelengths.

It is observed that UV region has a shorter wavelength than the IR region. The energy equation established by Plank and Einstein also known as quantum theory of light is given as, [1]

$$\mathbf{E} = \boldsymbol{h\upsilon}$$

$$\mathbf{E} = \boldsymbol{hc/\lambda} \qquad \text{Eq. (1.2)}$$

This shows that energy and wavelength are inversely proportional.

Hence because of the shorter wavelength, UV photons have more photon energy than IR photons and a smaller on-target spot size is achievable.

Why use UV lasers?

- First, they have a short wavelength (<400nm), which means that they can be focused to a small spot size (25 μm or less).
- Second, UV photons can get absorbed within fractions of seconds by the surface. This allows very fine control of the material removal process, especially when making blind features—features that do not go all the way through a material. Since there is less material removal per pulse, processing rates are slower. UV lasers also generally have a relatively short pulse length (<100ns) and this helps to achieve a high power density on the target.
- Finally, this high photon energy is enough to initiate bond breaking, especially in polymers containing π-electron clouds (double and triple bonds). The minimal thermal effects result in good edge quality. Hence they excel in processing of polymers.

Why use IR lasers?

- First, it is important to distinguish between near-IR (1 μm wavelength) and far-IR (10 μm wavelength) lasers. Even though both are IR lasers, they behave differently and interact with materials differently- some materials absorb better in the far IR and some absorb better in the near IR.
- IR lasers have relatively long pulse durations (microseconds to milliseconds) and wavelengths. A consequence of the long wavelength is that absorption occurs far into the material (sometimes hundreds of microns per pulse). These lasers are available in very high output powers—up to tens of kilowatts. Another consequence is that it is a first order thermal process because IR lasers interact with the rotation–vibration modes of molecules and thereby generate heat.

- Hence when it comes to costing, IR lasers are cheaper than UV lasers. Therefore they are best used when speed, part thickness, and large feature sizes are needed whereas UV lasers are best used when small spot sizes and good edge quality are more important than cost. [1]

CHAPTER 2

LITERATURE REVIEW AND OBJECTIVE OF PRESENT RESEARCH.

2.1. Literature Review

Laser marking being the latest and one of the most efficient marking technologies, there are a lot of research work that has been carried out over the past years on different fields. Similarly many research has been carried out in understanding the properties and applications of light metals and alloys. Literatures based on optimization technique, a very important tool for engineering applications are also numerous. The survey below are some of the collections of the work mentioned above mainly focussing on the field of laser marking.

Josefa and Gándara [9] have cited down the use and applications of Aluminium as the metal of choice in different industries. She has explained the important mechanical and physical properties of Aluminium which makes it an ideal material for use in aerospace, automotive, architechtural as well as domestic and other applications.

Lazov et al. [10] have presented a thorough study on different types of Laser marking methods that are available and its use according to the kind of requirements for the industrial applications. The different factors related to laser and the material that needs to be considered during the laser marking operation has been listed out and explained along with the type of lasers that are used. The use of laser marking application is increasing predominantly because of its flexibility, durability, repeatability and many other such benefits. There have been developments in this technology in order to lower operating cost and improve the mark quality at the same time for e.g. development of new green lasers for marking special products like silicon. Likewise other such developments have been implemented on this field.

Lazov et al. [11] have developed a methodology for automatic determination of contrast of laser marking since contrast is one of the main factors that determines the quality of laser marking especially during marking 1D and 2D barcodes. Laser marking of steel CT80 is done for the experiment using a fiber laser emitting at a wavelength of 1062nm .A raster marking method has been employed where the parameters taken for studying the effect on contrast is linear energy density and liner density of pulses . Range of values for these parameters were taken using their previous studies and raster marking was done for different combinations of these factors. Contrast was determined using Bulgarian State Standard 16383:1986 method.

Optimal values of linear energy density and liner density of pulses were obtained by eliminating those areas whose contrast were less. This study is beneficial for reaching optimal values of contrast more quickly.

Caiazzo and Alfieri [12] talks about simulating a moving laser heat source on aluminium alloy 2024 for the determination of heat generation and peak temperature at the fusion spot that leads to formation of a melt pool. A thin- disc laser source irradiating at 1030nm wavelength with a super Gaussian beam profile was used .Heat generation equations for a super Gaussian beam has been taken. Experiment has been performed taking some range of parameters to do the validation of the thermal model. Temperature at the fusion spot was measured using a two colour pyrometer and depth was also measured. These results were compared with the simulated results for those values of the parameters (scanning speed, Scan length, Power). With an average error below 4%, the model has been capable of predicting the depth of the fusion zone. Larger errors, of up to 16%, were found for the bead width instead; these will be addressed in future adjustments of the simulation.

Tam et al. [13] have studied the laser ablation phenomenon on Ni-Zn or Mn-Zn ferrite using a KrF excimer laser emitting at a ultraviolet wavelength of 248nm. The morphologies of the ablated surface was studied using scanning electron microscope. A glassy skin with a lot of micro-cracks was observed which could be removed by ultrasonic cleaning. The ablation threshold was found to be 0.3 J/cm^2 below which the laser radiation caused surface darkening or roughening causing the grain boundaries to become visible.

Conde et al. [14] has determined the temperature on the surface of the material during laser marking when the laser is irradiated perpendicular to the surface. They have taken an analytical approach for the temperature determination using Green function method. The simulation results show temperature distribution at different radial distance at different exposure times. For validating the model C02 laser having a wavelength of 10.6um has been taken for laser marking on methacrylate. Using profilometry and optical microscopy the HAZ depth, surface morphology and temperature distribution at different radial distance has been calculated. The results of the model and experiment show close correlation i.e., for increase in the exposure time ignition temperatures are reached that leads to changes in the structure leading to changes in the surface morphology as well as increase in HAZ. As the radial distance increases the temperature decreases on the surface shown by both the results. This model helps in determination of temperature at the surface leading to optimization of different processing

parameters i.e., Frequency v/s speed, Frequency v/s Power, Pulse width v/s Speed . The contrast was measured for each module using Image colour picker website and final analysis was done. Optimal values of frequency, scanning speed, Power and pulse width was chosen by checking the readability of the code done using a QR code scanner. For pulse width v/s speed, Low pulse width and low speed caused over-burning of the impact area because of high energy getting concentrated at the impact zone for a longer time .Hence the code was not readable. Correspondingly low pulse width and high scanning speed doesn't allow proper marking since the energy supplied could not get enough time for interaction with the material due to short pulse width. Hence marking with very low contrast was produced that is not readable. Hence optimum values of pulse width and speed and similarly other parameters needs to be selected such that the code is perfectly readable.

Tunna et al. [15] have investigated the interaction phenomenon occurring in Copper when irradiated by a high intensity laser radiation at 3 different wavelengths of 355, 532 and 1064nm using a Q switched Nd:YAG laser system. The etch rate observed for 3 different wavelengths at different intensities for each was observed. The morphological study was done by observing the formation of recast layer and oxides. SEM and optical microscopy was used for this purpose. The results showed that at highest wavelength of 1064nm, the etch rate was minimum as compared to that obtained for 355 and 532 nm wavelengths. Also on seeing the effect of intensity on etch rate, with the increase in intensity the etch rate increased considerably for a certain range and then after the saturation was reached. The reason for this was related to the nature of plasma formation on the surface of copper and the effects caused by it in terms of the recoil pressure. More absorption by plasma leads to more etch rate and vice versa. The formation of recast layer was also related to the intensity on the surface as well as the material properties. With the increase in intensity the melt expulsion velocity increased leaving lesser recast layer on the surface thereby reducing its height.

Araujo et al. [16] have studied the morphological changes appearing in Al 2024 when irradiated by a laser source. The fatigue test was done to study the crack formation. HAZ was studied using both optical microscopy and SEM. The results showed that on lower optical power, the thickness of the HAZ increased since with the increase in depth, Power decreases in-turn increasing HAZ. At the exit of the sample, molten material drips out due to pressure from the gas. This causes increases in HAZ at the bottom degrading the surface quality also affecting the fatigue resistance. The authors suggests to use another alloy of aluminium like 7475 or by

using high power laser source to decrease the effect of dripping of molten material at the bottom.

Qi et al. [17] studied the influence of pulse frequency on the mark width, depth and contrast on stainless steel marked using a Q-switched Nd:YAG laser source. . An optical microscope, scanning electron microscope and surface profile instrument were used for measuring the mark width and depth. The contrast was measured using an image-analysis system containing a frame grabber and a CCD device. SEM micrographs showed the image of laser marks at different frequency. The effect of frequency on mark depth and width was studied using graphs obtained from surface profile measurements. EDX spectrum showed the effect of frequency on the contrast. It was found that with the increase in frequency the mark width remained almost constant whereas the mark depth decreased after a frequency of 3Khz.The effect on contrast showed that with the increase in frequency the contrast increased as surface oxidation increased with the decrease in evaporation due to less peak power.

Lazov and Angelov [18] have done a parametric analysis to see the effect on contrast of laser marking. Raster marking of square field was done on carbon tool steel product. For the experiment fiber laser SP- 40P was used generating a wavelength of 1062nm having pulse width in the range of 8- 250ns. Experimental research methodology included mapping of a series of squares having side of 5 mm and making up a test field. Raster method was used for marking; its step being $\Delta x = 50$ μm. The parameters taken were: Scanning speed, Frequency and Power density .Single factor experiment was done where one parameters was varied at a time keeping the others fixed. Analytical relationship for determining contrast with respect to each parameter was developed using Lagrange equation of 3rd order. The results showed that with the increase in power density contrast increases. Optimum values of power density was chosen in terms of both visual and computer reading capabilities. With the increase in scanning speed contrast decreased and parabolic curve was obtained. Change in frequency did not have a significant effect on contrast. However deterioration in contrast is observed for frequency between 10-12 kHz since coefficient of overlap assumes negative value. (To obtain lines of proper sharpness and articulation, the coefficient of overlapping should have values within the interval $k0v \in [0, 100]$ %).

Chunling Li. [19] studied the effect of Laser marking data matrix on titanium alloy using Q-switched Nd:YAG laser emitting at a wavelength of 1064nm. ESEM and XRD analysis of the marked area was done to do the microstructural study of the marked zone. 2 data-matrix code

was marked on the titanium sample using 2 different current values i.e., 16A and 28A and the comparison was made. The ESEM analysis showed formation of re-solidified layers in both cases and the surfaces appeared rough. XRD analysis showed formation of micro-cracks on the sample marked with 28A current and hence it was proved that 16A current gave better marking results. The final conclusion made was that the nature of phases and structures of the titanium alloy was unmodified and hence it could be said that the effect caused by Q switched Nd:YAG laser was minimal.

Sobotova1 and Demec [20] have done a study on laser engraving stainless steel to study the effect of laser parameters like pulse frequency, scanning speed and number of repetitions on the visual changes and morphological changes on the material surface. Nd: YAG laser, emitting at a wavelength of 1064 nm was chosen for the experiment.32 squares with a defined pitch was marked varying these parameters. It was found that on increasing the pulse frequency and scanning speed lighter marks was obtained and the surface with more flat peaks were obtained. The effect of scanning speed was not much and on increasing the number of runs, more thermal effects were observed where the re-melting and re-solidification caused formation of structures with more heighted peaks.

Schille et al. [21] have investigated the effects of high pulse repetition ultra- short laser pulse laser system on certain processing criteria's for copper. The range of parameters of the laser chosen for the investigation were Pulse power, pulse frequency, pulse energy, wavelength and pulse duration and the processing criteria's studied were ablation rate, material removal efficiency and productivity. The machining quality in terms of surface roughness was also measured using surface roughness measurement and SEM. The maximum average power of 31.7W was applied and the pulse repetition rate was ranged between 200Khz - 20Mhz corresponding to which the pulse energy ranged between 1 to 50um. The results showed , higher ablation rate for shorter wavelength lasers and the volume ablation rate increased for higher fluence while frequency had no significant effect on the ablation rate. On increasing the pulse duration, the ablation rate decreased and roughness increased due to appearance of micro-melt structures and smoother surface was obtained while using pulses of low pulse energy.

Li. et al. [22] have done a research on laser marking 2D codes on surfaces of aluminium alloy using raster marking method. They found out that the edge over-burn effects that hampers the readability of miniature DM codes are minimized using this method. Temperature field model was developed in order to study how the contrast and print growth are affected during laser

material interaction. For the experiment purpose 3 processing parameters were taken i.e., Q frequency, average power and repeat scanning number. The threshold power and frequency obtained from the experiment was 3.6 W and 110 KHz. The test results showed that the average power and frequency have the most influencing effect on the contrast and print growth. Single factor experiment keeping one parameter fixed and varying the other was carried out to see the effect of the aforementioned parameters on the shape/size and appearance of the module marked. The effect of repeat scanning number is not as much as the other two parameters. In addition, Ultrasonic cleaning greatly improved the readability of the miniature code.

Velotti et al. [23] have performed a comparative study on laser marking of titanium alloy and titanium sheet that is used in aerospace industries. They have tried to do a parametric analysis taking parameters Pulse energy, scanning speed and pulse power on the marking geometries (depth and width). Certain range of values for these parameters were taken and single factor experiment was performed. For the experiment titanium particles were deposited on aluminium alloy and titanium sheets were also laser marked to do a comparative study .A 30 W MOPA Q-switched Yb: YAG fiber laser was used. The mark appearance obtained for different combinations of these parameters were studied and the window for the parameters that created a regular and effective mark appearance was chosen for further analysis. The effect of scanning speed on the mark depth and width at different pulse power was studied and compared for both the cases. The geometry of the groove was measured using a HIROX HK9700 optical microscope. It was found out that the processing window for both the cases were nearly the same. However mark depth for coating was much higher than the sheet.

Svantner et al. [24] have studied the effect of laser marking on the corrosion resistance of austenitic stainless steel AISI 304. Pulsed fiber laser SPI G3 having average output powers 20 W, 30 W, and 40W of various focal lengths were used for laser-marking experiments. The analysis carried out were corrosion tests, roughness, microscopic and chemical analysis, energy dispersive x-ray, grazing incidence x-ray diffraction, and ferrite content analyses were carried out. The results showed improvement in corrosion resistance when the heat input was low as the amount of oxide present was low. Along with this pulse length and pulse frequency also affected corrosion resistance. Lower pulse length and higher pulse frequency improved corrosion resistance. GIXRD analysis was carried out to find a correlation between ferritic and oxide content and the results showed that lower ferritic content with lower oxide content improved corrosion resistance.

Li et al. [25] studied the effect of process parameters (current intensity, scanning speed, frequency and fill spacing) on the quality of barcodes laser marked on the surfaces of aluminium alloy 6061 using a Q-switched lamp-pumped Nd: YAG laser with a wavelength of 1064 nm. Single factor experiment was done using range of process parameter values and surface roughness was calculated and its effect on the image grade was studied using plots. Taguchi DOE was done using the range of values from single factor experiment which is most significant and the experiment was performed accordingly to find the optimum values of the parameters. Confirmatory experiments was performed to match the results obtained from Taguchi method. Here was a good match between the two results. ANOVA was done to obtain a predictive model for determining the surface roughness of 2D code. Experiment was done to validate the model and the results obtained closely correlated with the model results proving its effectiveness.

Li and Lu [26] have studied the effect of certain process parameters on the contrast and surface roughness during laser marking data-matrix code on the surface of TC4 titanium alloy plates using Q switched lamp pumped Nd: YAG laser. The process parameters taken were current intensity, scanning speed, frequency and scanning space. Single factor experiments were performed in order to study the effect of these parameters on the contrast and surface roughness using range of process parameter values. Taguchi L25 orthogonal array DOE was used to find a co-relation between the symbol contrast and surface roughness. The surface roughness of each Data Matrix symbol was measured using a TR200 hand-held surface roughness instrument and symbol contrast was obtained using a program written in MATLAB. The results of the single factor experiment showed that the effects were non-linear and hence multivariate non liner regression analysis was done and predictive model for determining the surface roughness was developed. In order to check the validity of the model experiments using the orthogonal array data was performed and a comparison between actual and predicted values of the roughness was obtained .The results showed close similarity between the two and the model developed was found to be statistically significant.

Bahaudin et al. [27] have investigated the effect of Laser processing on the surface morphology as well as the changes in the chemical composition of Copper using a Q- switched Nd:YAG laser. Analysis on the surface roughness was done using SEM and the changes in chemical composition was studied using EDX analysis. The laser was irradiated on the copper surface using 2 different energy levels as 224 and 465 mJ and comparison between these two energy levels was done. On irradiating the laser, formation of ripples with porosity, pits and micro-

cracks was observed. On increasing the energy level roughening increased and rapid solidification lead to the solidification growth. Increase in roughening was due to the highly energetic beam effect leading to high pressure shock waves that causes surface tension gradient leading to formation of ripples. EDX analysis showed increase in oxygen level on increasing the energy due to the oxidation effect taking place and decrease in carbon percentage due to laser ablation that causes burning of carbon removing it from the surface.

Manda et al. [28] have studied the effect of 3 process parameters i.e., scanning speed, frequency and Laser power on the 3 process criteria i.e., kerf width, surface roughness and HAZ .For the experiment they have taken Nd:YVO4 laser and the material chosen was aluminium alloy 707. Taguchi DOE they used Taguchi DOE for reducing the number of experiments. S/N curves was generated to study the effect of the process parameters on the responses. Optimization of the process parameters was done using Taguchi methodology and confirmatory experiments were performed to validate the results and it showed close correlation between the actual and predicted values of the responses. It was found that with the increase in Power and Frequency, HAZ and kerf width increases but with the increase in scanning speed it reduces due to insufficient heating. With the increase in Power surface roughness increases but with the increase in scanning speed it decreases. With the increase in frequency surface roughness first decreases but with further increase in frequency it increases. SEM was used for microstructural analysis and AFM was used for surface roughness analysis.

Fraser et al. [29] carried out a study on laser marking performance obtained on different non-ferrous metals like tin, lead, nickel, aluminium, titanium and zinc. Since these metals hold a great application in industries which require light weight metals for e.g. aerospace, automotive etc. marking on these materials for product traceability is required by many producers. In this study laser marking a matrix of squares on each metal has been done using a Q-switched fiber laser emitting at 1064nm wavelength having a beam spot diameter of 90 um on the surface. The parameters changed during this matrix marking we dill spacing and scanning speed. For each metal matrix marked, that resulted in best contrast was chosen for further studies. From this best contrast mark, the morphological studies was done or each metal which showed that for lead and zinc large line spacing resulted in high contrast mark whereas for tin, lead and nickel very less line spacing resulted in dark marks. The relationship between contrast and marking speed was studied which showed that aluminium (0.96 cm^2/s) had the least marking speed and lead had the highest marking speed (2.79 cm^2/s) to obtain a contrast of 100. Further possible studies under this topic has been noted by the researcher.

Naumova et al. [30] has performed a study on colour marking on the surfaces of copper alloy. They have studied the effect of different laser parameters on the colouring contrast of the image. For the study an L60 brass plate was chosen as the base material and Ytterbium fiber laser was used as the laser source. The topology of the surface was obtained using a secant method which was done using an HVS-10 Vickers hardness tester equipped with a special microscope eyepiece. The colour assessment was done using a Canon EOS 5D Mark III camera. The colour identification was done using RAL (from German Reichsausschuß für Lieferbedingungenund Gütesicherung) color chart. Correlation between topology of the surface and formation of specific colour groups was done .The laser parameters chosen were pulse energy, scanning speed and defocussing. Its effect on the formation of specific colour groups was done .It was found that by adjusting the distance between lines during scanning, a certain uniform colouring can be obtained on the surface.

Kucera et al. [31] developed new method for time resolved surface temperature measurement during laser marking for studying the changes in microstructure, phase composition and test corrosion resistance. The material used was stainless steel and laser marking system used was nanosecond pulsed fibre laser with variable pulse duration (from 9 to 200 ns), repetition frequency and pulse energy. Three sets of laser parameters were used for doing the analysis based on previous work. For doing the corrosion test Double Loop Electrochemical Potentio-dynamic Reactivation Technique (EPR-DL) was used to detect susceptibility to inter-granular attack associated with precipitation of chromium carbides at grain boundaries. The changes in surface morphology of the near-surface layer was carried out using a Grazing incidence X-ray diffraction technique (GIXRD). The surface phase composition of the as-received and laser treated samples was evaluated by GIXRD analysis. The time dependence of the surface temperatures for various laser setting parameters was done and effect of pulse energy on temperature while keeping scanning speed and pulse duration fixed and effect of scanning speed on temperature while keeping pulse energy and pulse duration fixed was done. The results showed strongly reduced corrosion resistance is obtained for process No. 3, with the highest measured temperature which perfectly agreed with the cross section observed from SEM analysis. This measurement method enabled comparison of different processing parameters and helped the understanding of processes during pulsed laser processing of material, including melting, the cooling rate and the heat accumulation effect.

Leone et al. [32] have done the investigation on the effect of different process parameters on laser marking of Inconel 718 using a 30 W Q-switched Yb: YAG fiber laser. Parameters were

chosen based on the theoretical knowledge on obtaining the best laser marking results. The responses chosen were the mark geometries (width, height) and contrast .Changes in the mark geometries on changing the frequency while keeping average Power and scanning speed constant were studied through experiment. Methodology for determining the Weber contrast was adopted based on the grey values. Statistical methodology was used to analyse the effect of the process parameters, provide a predictive model of the process and optimise the process conditions. Response Surface Method (RSM) was used to provide statistical model which is able to describe the behaviour of geometry and the Contrast as a function of the process parameters. To find the optimal conditions for obtaining best laser marking results, the Master Response Optimization (MRO) technique was incorporated. The results showed that the average power and the linear energy play an important role in the mark geometry formation (all the geometrical features increase at the increase of Pa and Le).Also the frequency has its contribution in the formation of the mark geometry, the decrease in frequency, involves an increase of the pulse power (or equivalently the pulse energy), and hence triggers the keyhole phenomenon.

Roy et al. [33] have studied the effect of chosen parameters i.e. power, scanning speed and frequency on mark depth and width during laser marking. Laser marking on AISI304 stainless steel using Nd-YVO4 laser generating at 1064nm wavelength was done. Response Surface methodology was used to find optimum values of the parameters for obtaining minimum mark width and maximum mark depth. Contour plots and surface plots were made to study the effect of the process parameters on the responses. The conclusions made were Increase of laser power usually gives more heat energy, and hence, increases mark width and depth. • Increasing scanning speed decreases mark width and depth because of less heat input to the marking region. • Maximum mark width and mark depth can be obtained at a when laser power of 6.96 W, pulse frequency of 16.69 kHz and scanning speed of 6.60 mm/s.

Shivakotia et al. [34] have carried out laser marking on Gallium nitride using a diode pumped Nd:YAG laser to study the effect of 3 process parameters(current, scanning speed and frequency) on the geometrical features of laser marking as well as the intensity .RSM DOE was used to generate a list of combination of parameters for experimentation purpose . Responses were measured accordingly and a predictive model was developed that correlated the process parameters with the responses. For testing the significance of the model ANOVA was done and the results showed a lack of fit of 5.4% with 95% confidence interval which is acceptable. Verifying experiments of the model was done using different combination of

parameters and prediction error were calculated which was again within the acceptable limit. RSM based Multi-objective optimisation was done to obtain the best combination of parameters that gave minimum mark width, maximum depth and intensity. Again a verifying experiment was performed using those set of parameter values and the responses were calculated and compared with the predicted values and prediction error was calculated which was within acceptable limit. Sensitivity test was done to obtain that parameter which has significant effect on the responses which showed that that current and pulse frequency have most significant contribution for varying the mark width, mark depth and mark intensity.

Murzin et al. [35] studied the effect of femtosecond laser pulses on the surface of copper surface on irradiating it with an energy density below the ablation threshold while moving the sample in a particular direction. This resulted in appearance of different colour on the surface of copper sample on changing the direction of movement of the sample the colours were classified into 3 types: blue-turquoise, red-violet, orange and grey-green. Images of the treatment zones were obtained using metallographic optical microscope. Atomic force microscopy was used to see the surface topology of the different coloured areas of the sample. Low spatial frequency surface structures were formed. Height profiles of the different coloured areas were also measured which showed that even small changes in the nanostructures lead to colour changes. FEM quanta 200 SEM was used to examine the laser processed tracks. Spherical adhered particles were observed majorly on the red-violet region than on the blue-turquoise region. These particles were identified as copper oxide. Secondary and backscattered electrons SEM images were taken which showed that the region corresponding to brighter images were due to lower presence of oxygen and higher content of copper. There were the possible reasons for the change in colour of the surface during laser marking.\

Li et al. [36] has studied the effect of process parameters(pulse frequency, Power and scanning number) on the readability of 2d code laser marked on 50CrVA stainless steel using an industrial Q-switched fiber laser (YLP-D10 by Hans laser), working at the fundamental wavelength of 1064 nm. Numerical model was developed to study the effect of temperature field on the contrast and print growth that affects the readability of the code. Simulation results fetched values of threshold intensity, frequency and average power. These results were validated through experiment where raster marking was done for different combination of process parameters. The contrast, print growth and the threshold values of frequency and average power were measured from this experiment and compared with the simulation results. The results matched well. Optimisation of process parameters was done using single factor

regression analysis. With the help of statistical graph effect of process parameters on print growth and contrast was studied. It was concluded that temperature change in depth direction and oxidation degree of laser radiation are main reasons for contrast of DM code and temperature change in radius direction is the main reason for print growth. Additionally ultrasonic cleaning greatly improved the reading quality of miniature code and corrosion resistance was improved by covering a layer of polyurethane coating.

Pavels et al. [37] has done a research on laser marking QR code on plastic ABS to obtain optimum values of process parameters (frequency, scanning speed, Power and pulse width) that gives perfect readability of the code marked. Marking was done using The Rofin PowerLine F20 Varia Laser System. It is a fiber laser with a wavelength of 1064 nm. Raster marking was done where a 10*10 matrix was prepared and was laser marked for different combinations of 2 parameters each. Total of 3 different experiments were performed taking the following combination of parameters.

Sun et al. [38] has implemented a method of laser marking which helps improve the precision, processing quality and recognition rate of the mark. He has used a method for dot-matrix marking with femtosecond laser on nickel-based alloy using diaphragm modulation. The titanium Sapphire solid femtosecond laser, having 120-fs-width pulse with the maximum pulse energy of 4 mJ was used. The frequency and wavelength of 1 kHz and 800 nm respectively was used. First experiment was performed without defocussing. The results showed significant melt and spatters on the edge of the craters of nickel-based alloy GH4169 under laser ablation at the focal point. In order to solve the problems of poor morphologies and small size at the focal point, they proposed a method to obtain marking units with diameters of 300-500 um using femtosecond defocused pulses. The results showed that the morphological quality and the diameters of the craters increase significantly after defocusing ensuring the reliability and durability of the marking. The parametric study was also done to check how each parameter affect the depth and diameter of the craters formed. The parameters chosen were Pulse energy, pulse number, the diaphragm size and the amount of defocussing. The appropriate range of the diaphragm size obtained was from 8 to 10 mm. With the addition of the diaphragms, the regular variation of the diameters of the craters under different parameters was beneficial to control the size of the marking units. As a result of the edge diffraction, the melt phenomenon on the edge of the marking units almost disappeared, so the boundary of the crater was clear. Moreover, the laser energy was periodically distributed due to the diffraction effect of the diaphragm, which was conductive to the formation of highly uniform microstructures. The

decrease in the difference of gray value within the crater decreased by 60 lead to the improvement in recognition uniformity and the recognition rate of the marking. Contamination test was done to check the recognition rate after adding the diaphragm. Furthermore, the cracks and re-cast were not observed by metallographic analysis. Therefore, with spatial shaping of laser beam by the addition of diaphragm, the femtosecond laser marking technology has the advantage of high position precision, dimensional accuracy, processing quality and recognition rate.

Du et al. [39] have investigated the effect of single pulse energy on surface roughness of Al2024 alloy by dividing it into many levels using the control variable method. For the experiment AF20 MOPA Fiber laser emitting at 1060nm wavelength was taken. SEM test were done in order to study the composition and morphology of the laser irradiated surface. In order to study the effect of single pulses, the laser was irradiated using different waveform and the relation between different waveform and roughness was derived graphically. The results showed that with the increase in waveform, the pulse energy decreased and the surface roughness decreased. The reason being with the decrease in pulse energy, energy available is not high enough to melt and vaporize the material that results in the formation of dense and spherical particles on the surface which appears as recast layer after solidification. Lower and lower materials melt and vaporize and the energy is insufficient to eject out the materials resulting in the formation of only small pits. SEM and EDM analysis showed that melting, vaporization and re-solidification lead to the formation of oxides and oxygen content. It was concluded that parameters like fill spacing, scanning speed, frequency, etc., affect the amount of oxidation to a large extent.

Atanasov and Lengerov [40] have done a research on increasing the efficiency of laser marking by double writing the symbols. They have taken Aluminium 1050 sample and the laser source used was a CuBr Laser emitting at a green wavelength of 511nm. Experiment was performed by varying 2 parameters i.e., scanning speed and repeat scan number. They showed the dependency of reflection coefficient with the number of laser scans whose result showed that with the increase in the number of laser scans the intensity ratio decreased which means increase in contrast. Similar relation between the intensity ratio and scanning number was done which showed that with an increase in scanning speed the intensity ratio increased which means reduction in contrast. Reasons for above results were explained. This research has the capability of improving the productivity of laser marking with good quality marks.

Lazov et al. [41] have studied the influence of some laser parameters like power density, frequency and effective energy on the contrast of laser marking for different values of scanning speed. The material used was carbon structural steel 15Cr2, using a fiber laser. The relationship between other parameters that directly affect the output along with power density have been given in the form of equations. After studying the trend on the output, the operating range of the target parameters have been chosen. Using this range, laser marking barcode, 2d codes and company logo was done where the objective was to test the readability of the marked codes visually/digitally.

Montero et al. [42] has implemented a new laser marking system which is capable of producing multiple laser beams by using a series of Laser diodes in order to increase the production line speed upto 16m/s hence overcoming the barrier of production bottleneck caused by laser marking system irradiating a single beam capable of completing the operating with a maximum speed of 8m/s. They have developed and tested two laser marking solutions for two different application requirements: (1) fiber-coupled Laser Diode Array (f-LDA) technology for high-speed and high-resolution printing, using thermo-chromic pigments; and (2) High Power fiber-coupled Laser Diode Array (HP f-LDA) technology for very high-speed coding. The parameters and values for both the systems have been selected accordingly. The speed achieved by this system is the highest speed achieved so far for any laser marking system.

Hamadi et al. [43] have performed a statistical study to investigate the effect of 4 laser parameters on the marking of pure Titanium substrate using a Q switched frequency doubled Nd:YAG green laser that emits at a wavelength of 532nm operation with a short pulse duration of 5ns. They have used a fractional factorial DOE to perform minimum number of experiments with maximum precision. The parameters taken were pulse frequency, pumping energy, scanning speed and line spacing and the responses they have taken were Surface roughness (Ra) and Surface brightness (SB).Surface roughness was tested using VISION model profilometer and Surface brightness was tested using Minolta calorimeter. On analysing the results they found out that scanning speed and spot diameter had the maximum influence on the results. Increase in scanning speed let to decrease in Ra and decrease in surface brightness and increase in spot diameter let to increase in Ra. Optimisation of values were also done considering the objective as decreased surface roughness and increased surface brightness.

Conde et al. [44] have performed a numerical and experimental study for studying the formation of different structures upon laser irradiation on the surface of Titanium alloy using

and Nd:YAG laser emitting at a wavelength of 1064nm having a beam diameter of 60um.The numerical simulation was done in order to study the temperature gradient on the material which is beneficial for studying the changes in the macrostructure. From the FEM analysis done in ANSYS software, the relation between the crater depth, aspect ratio temperature, time and distance from the beam spot was established .The time at which the boiling and melting temperatures are obtained from it and the number of laser pulses which leads to structures changes and HAZ profiles are obtained as well. Experiment was performed to check the validity of the model established and close correlation was obtained between the two.

2.2. Objective of Present Research

Research gap

After a thorough survey of the work that has been carried out so far in laser marking, it is observed that there are a very few work in which investigation of the process parameters while marking on pure Aluminium and Beryllium Copper has been carried out. These materials have a huge demand in many industries like aviation, automotive, electronics, oil and gas industries as well as in domestic applications because of its useful electrical, thermal and most importantly mechanical properties like high thermal and electrical conductivity, high strength to weight ratio, high fatigue strength, high corrosion resistance, etc. Hence it is important to understand how these materials behave when laser processed and marking being one of the most efficient, cost saving and permanent marking technology having demand in all the above mentioned industries for product tracking and identification, efficient marking on these materials is as important. Hence this thesis aims at investigating the effect of some of the process parameters on the process responses which is surface roughness and heat affected zone of Aluminium and Beryllium copper. The reason for choosing these two process responses is because in marking, the quality of the mark is assessed through many criteria's out of which contrast and print growth is one of them and one of the factors that affect contrast is surface roughness. Similarly heat affected zone is one such factor that affects print growth. Controlling these two can help achieve a good quality, easily identifiable marks.

Objective

Keeping in mind the above research gap, the objective of this research is summarized below.

i. To study the mechanism of laser marking and identify the principle process variables.
ii. To study the features and operational parameters of a Multi –Diode Pump Fiber Laser marking system.
iii. To perform trial experiments on Aluminium and Beryllium Copper to determine the working levels of the parameters and to plan detail experimentation using appropriate statistical tools.
iv. To investigate the effect of process parameters i.e. Power, scanning speed and frequency on two process criteria's i.e. the Surface Roughness (Ra) and Heat Affected Zone (HAZ) in marking of Aluminium, a light metal.
v. To study the effect of input process parameters i.e. Power and Scanning speed on two process responses i.e. the Surface Roughness (Ra) and Heat Affected Zone (HAZ) in marking of Beryllium Copper, a light metal alloy.
vi. To develop a mathematical model using Regression analysis for predicting the values of the responses and to carry out ANOVA test to check the efficacy of the model obtained.
vii. To optimize the process parameters using Multi objective Particle Swarm Optimization (MOPSO) technique for obtaining the best combinations of process parameter values to maximize surface roughness and minimize heat affected zone for different laser marking applications.

CHAPTER 3

EXPERIMENTAL SETUP AND METHODOLOGIES

3.1. Experimental Setup

The marking experiment was carried using a Multi-Diode Pumped Fiber Laser Marking machine emitting at a wavelength of 1064nm which falls under infrared region of the electromagnetic spectrum and having an average power of 50W. It operates in pulsed mode because of which the maximum peak power obtained can reach up-to 7.5 kW which makes this machine capable of performing many high powered laser applications like cutting, drilling, grooving, channelling, etc. Other applications achievable by this machine include marking, surface texturing and colour changing. The specifications of the machine is given in table 3.1 below.

Table 3.1. Specifications of Diode Pump Fiber Laser Marking machine

Parameters	Specifications
Laser type	Multi Diode Pump Fiber Laser
Laser manufacturer	Sahajanand Laser Technology Ltd.
Model no	SCRIBOSCF175
Class	4
Software	I-MARK (version 8.4.1)
Nominal average Power	50W
Pulse repetition rate	50-120 kHz
Mode of operation	Pulsed mode
Laser beam spot diameter	21um
Beam mode	Gaussian mode
Wavelength	1064 nm
Pulse duration	120ns
Focal length	75 mm

The components of the Diode Pump Fiber Laser machine are as follows:

a) Laser head
b) Optical fiber

c) Collimator
d) CCTV and CCD
e) Beam delivery unit and Beam bender
f) F theta focussing lens
g) Servo control X-Y worktable
h) Assist gas supply unit

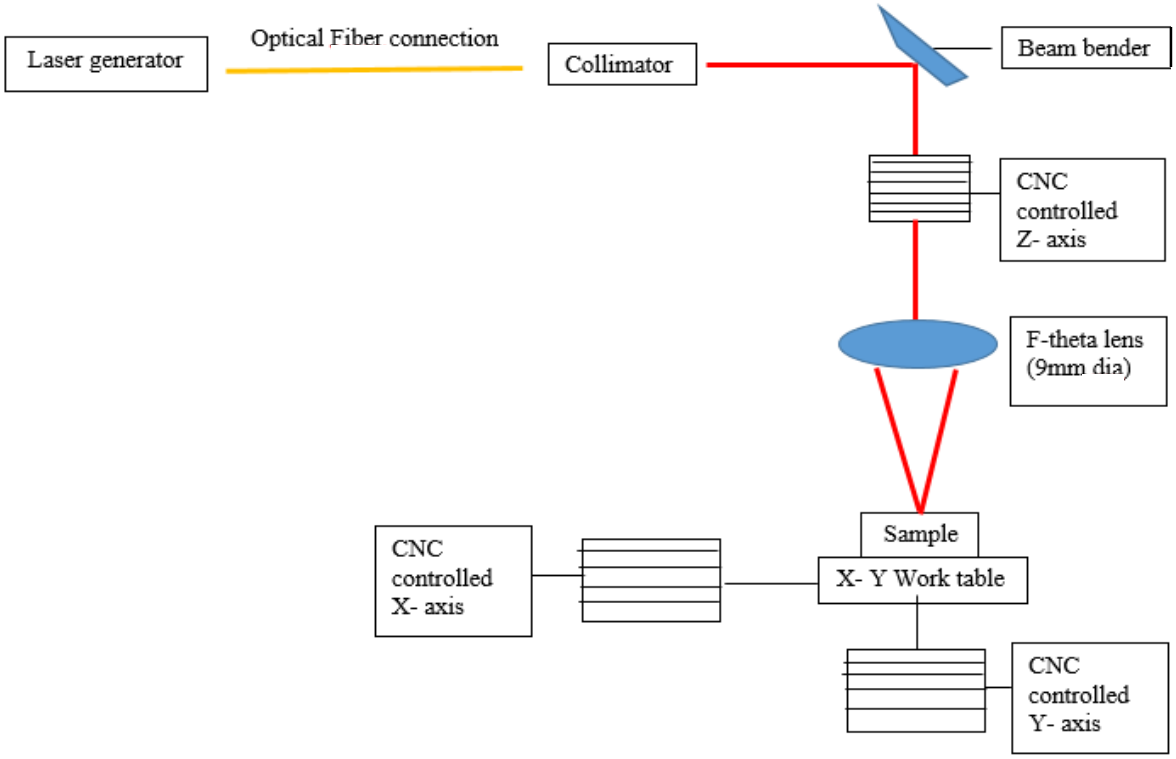

Fig. 3.1. Diode Pump Fiber Laser marking components

The CNC controlled worktable has a working area of 150*150 mm² and the servomotor can be allowed to vary from 0.1- 30mm/s for X, Y and Z axis. The specifications of the worktable is given in the table below.

Table 3.2. Specifications of CNC work table

Worktable	CNC controlled
Axis of travel(X and Y) (maximum working area)	150 *150 mm²
Resolution	1 um
Clamping of work-piece	Developed fixture
Feed rate	0.1-30mm/s
Control loop system	Open loop control

3.2. Experimental Procedure

Machine start-up:

1. The main power supply is switched on.
2. If assist gas is required then the main switch connected to the compressor is turned on.
3. The lever present on the bottom left of the machine is pulled up. This turns the marking machine on.
4. Now to operate the PC and CCTV, the UPS and CPU is turned on. The PC and CCTV gets connected.
5. Finally the "on" button of the CCTV is pressed to view the machining taking place. The process is captured with the help of CCD which is connected to the CCTV.

Step 1 and 2 Step 3

Step 4

Step 4 Step 5

Fig.3.2. Diode Pump Fiber Laser Marking machine in Operational mode.

To begin the operation:

1. To clamp the sample, first the safety door is opened.
2. The fixture is slid out and the sample is clamped manually.
3. The fixture with the sample is placed back and the safety door closed.
4. Now the “I- MARK” software on the PC is opened. The screen will be displayed as shown below.
5. The program for the required operation is uploaded .
6. The step value on the monitor is provided and “Jog” mode is selected to move the cursor to the desired position for starting the operation.
7. With the help of the arrow keys on the keyboard, the position on the sample from where the operation needs to be started is fixed. The magnified image of the sample showing the position being chosen will be displayed on the CCTV.
8. After finalising the position the X and Y position values obtained manually from jog mode is inserted to the software in order to give the current position as the start position to the laser and “Enter” button is pressed. The position gets locked on the software.
9. The values of Power, Scanning speed, frequency and duty cycle is inserted in the space on the screen corresponding to the respective parameters accordingly and “update” is done.
10. Now the operation is started by clicking on “Start F2” option. The marking begins.
11. These steps are repeated for the corresponding experiments.

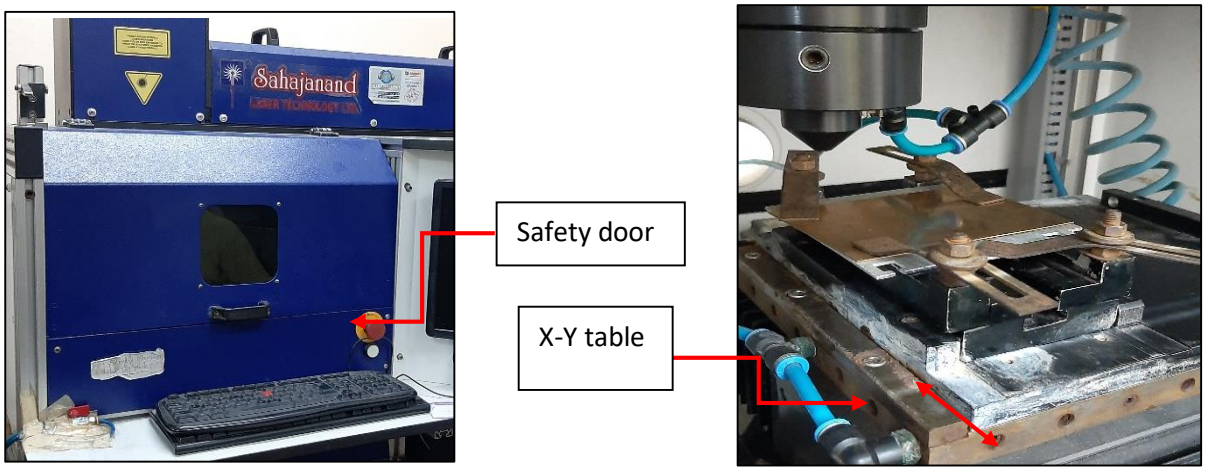

Step 1 Step 2 & 3

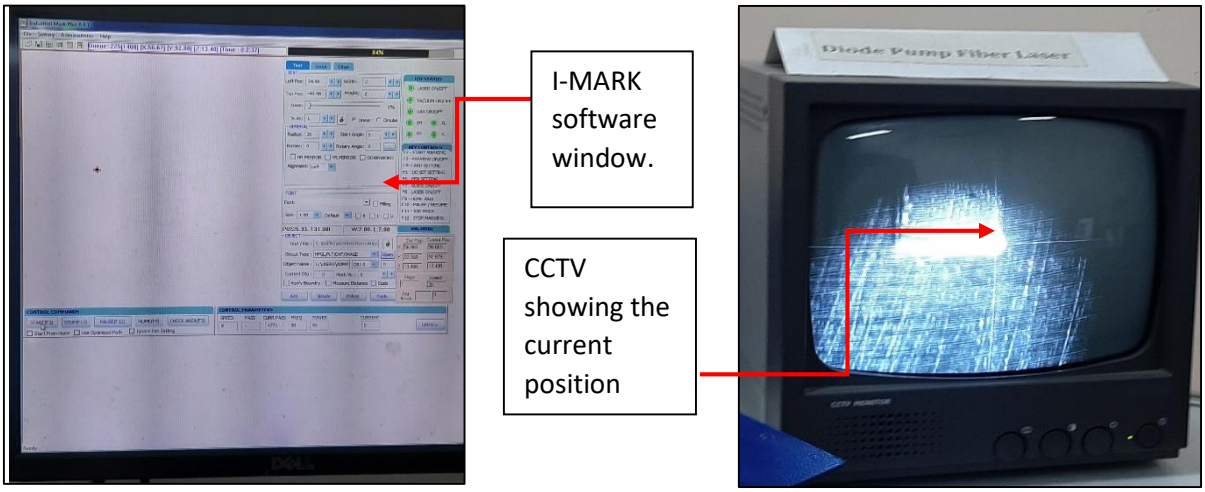

Step 4, 5& 6 Step 7

Fig. 3.3. Laser marking operation

3.3. Optimization Technique

Introduction

Optimization is the process of obtaining the best solution out of many solutions under certain circumstances i.e. subjected to constraints. It is a very important tool used in engineering applications for obtaining the best possible solution to any problems. The process is classified into two categories [45]:

i. Traditional optimisation technique
ii. Non- traditional optimisation technique

There are several methods under each category and those are selected depending on the kind of problem one faces. Some of the methods under both categories are listed below.

i. Traditional method- Classical techniques (Lagrange multiplier), Numerical methods, Bracketting method, Region elimination method, interpolation method, etc.
ii. Non- traditional technique- Particle Swarm Optimisation, Genetic Algorithm, Simulated Annealing.

Brief discussion on Non- traditional Optimisation technique

Non- traditional techniques are conceptually different from the traditional techniques. These are nature inspired techniques i.e. based on certain characteristics and behaviour of biological, molecular, swarm of insects and neurobiological system [45].

The features of this algorithm are as follows:

a) A population of points (trial design vectors) is used instead of a single design point.

b) Since several points are used as candidate solutions, less likely to get trapped at a local optimum. It gives Global optimum.

c) They use only the values of the objective function. The derivatives are not used in the search procedure.

d) The design variables are represented as strings of binary variables and is applicable for solving discrete and integer programming problems. For continuous design variables, the string length can be varied to achieve any desired resolution.

e) The objective function value corresponding to a design vector plays the role of fitness.

This method can be further classified into two types:

i. Behaviourally inspired algorithm- Particle Swarm Algorithm
ii. Evolution based procedure – Genetic Algorithm

Particle swarm Optimization technique

Particle swarm optimization, abbreviated as PSO was originally proposed by Kennedy and Eberhart in 1995 [45]. It is based on the behavior of a colony or swarm of insects, such as ants, termites, bees, and wasps; a flock of birds; or a school of fish. The particle swarm optimization algorithm mimics the behavior of these social organisms. The word particle denotes, for example, a bee in a colony or a bird in a flock. Each individual or particle in a swarm behaves in a distributed way using its own intelligence and the collective or group intelligence of the swarm. As such, if one particle discovers a good path to food, the rest of the swarm will also be able to follow the good path instantly even if their location is far away in the swarm.

Working principle of PSO

In the context of multivariable optimization, the swarm is assumed to be of specified or fixed size with each particle located initially at random locations in the multidimensional design space. Each particle is assumed to have two characteristics: a position and a velocity. Each particle wanders around in the design space and remembers the best position (in terms of the food source or objective function value). Each particle is assumed to have two characteristics: a *position* and a *velocity*. Each particle wanders around in the design space and remembers the best position (in terms of the food source or objective function value) it has discovered. This best position obtained by each particle is known as local best or "p-best". This position is always stored in the memory/ archive.

The particles communicate information or good positions to each other and adjust their individual positions and velocities based on the information received on the good positions. Position of individuals are modified based on own experience and collective experience (swarm experience). The position modified by each particle based on collective information is known as global best or "g-best". Information obtained are used to find out best direction towards optimum [46].

Based on the number of objective functions PSO is classified into:

i. Single objective – only one objective function.
ii. Multi objective – two or more and often conflicting objective functions

Multi objective Particle Swarm Optimization (MOPSO)

When there are two or more and often conflicting objective functions, it is known as Multi objective optimization [47]. For e.g.

Problem statement- Buying a car

Objective – Minimize cost and maximize comfort

In MOOP, the goodness of a solution is determined by its dominance. There are conflicts between the objectives and hence finding a single solution satisfying all the objectives is not possible. Therefore it operates by obtaining a non-dominated Pareto solution also known as a Pareto optimal set, in which there is a tradeoff between the multiple objectives. The mapping of these Pareto set is known as Pareto front. The quality of the final solutions is evaluated by the convergence and diversity criteria of these Pareto set [47].

Computational Procedure of MOPSO

The optimization used for the current thesis is an unconstrained Multi-Objective Particle Swarm Optimization (MOPSO). The computational procedure it follows is discussed below [45,46] .

i. The multi-objective function f(X) is provided.

ii. The range for the variables of the objective function to be optimized i.e. lower limit and upper limit is provided.

iii. The number of particles or size of the swarm as 'N' is set.

iv. The initial population of $\mathbf{X}$ in the range $\mathbf{X}_{(l)}$ and $\mathbf{X}_{(u)}$ randomly as $\mathbf{X}_1, \mathbf{X}_2, \ldots, \mathbf{X}_N$. is generated.

Hereafter, the position and velocity for each particle in 'i'th' iteration are generated using the governing equations of PSO and are denoted as $\mathbf{X}_{j\,(i)}$ and $\mathbf{V}_{j\,(i)}$ respectively. Thus the particles generated initially are denoted $\mathbf{X}_{1(0)}, \mathbf{X}_{2(0)}, \ldots, \mathbf{X}_{N(0)}$. The vectors $\mathbf{X}_{j\,(0)}$ $(j = 1, 2, \ldots, N)$ are called particles or vectors of coordinates of particles.

v. The velocities of particles are found. All particles will be moving to the optimal point with a velocity. Initially, all particle velocities are assumed to be zero.
The iteration number is set as i = 1.

vi. $\mathbf{P}_{best}$ and $\mathbf{G}_{best}$ are computed. $\mathbf{P}_{best,j}$ and $\mathbf{G}_{best}$ are two points found so far (upto i^{th} iteration) having good objective function value (closer to optimum value). Displacement (velocity) towards these points will improve the objective function value.

vii. If the positions of all particles converge to the same set of values, the method is assumed to have converged.

viii. If the convergence criterion is not satisfied, step v. is repeated by updating the iteration number as i = i + 1, and by computing the new values of **P**-best, j and **G**-best.

ix. The iterative process is continued until all particles converge to the same optimum solution or after a fixed number (large) of iterations.

x. The global best solution in each iteration is the best solution and after convergence the last global best solution is accepted as optimum solution.
Below flow chart shows the algorithm for MOPSO.

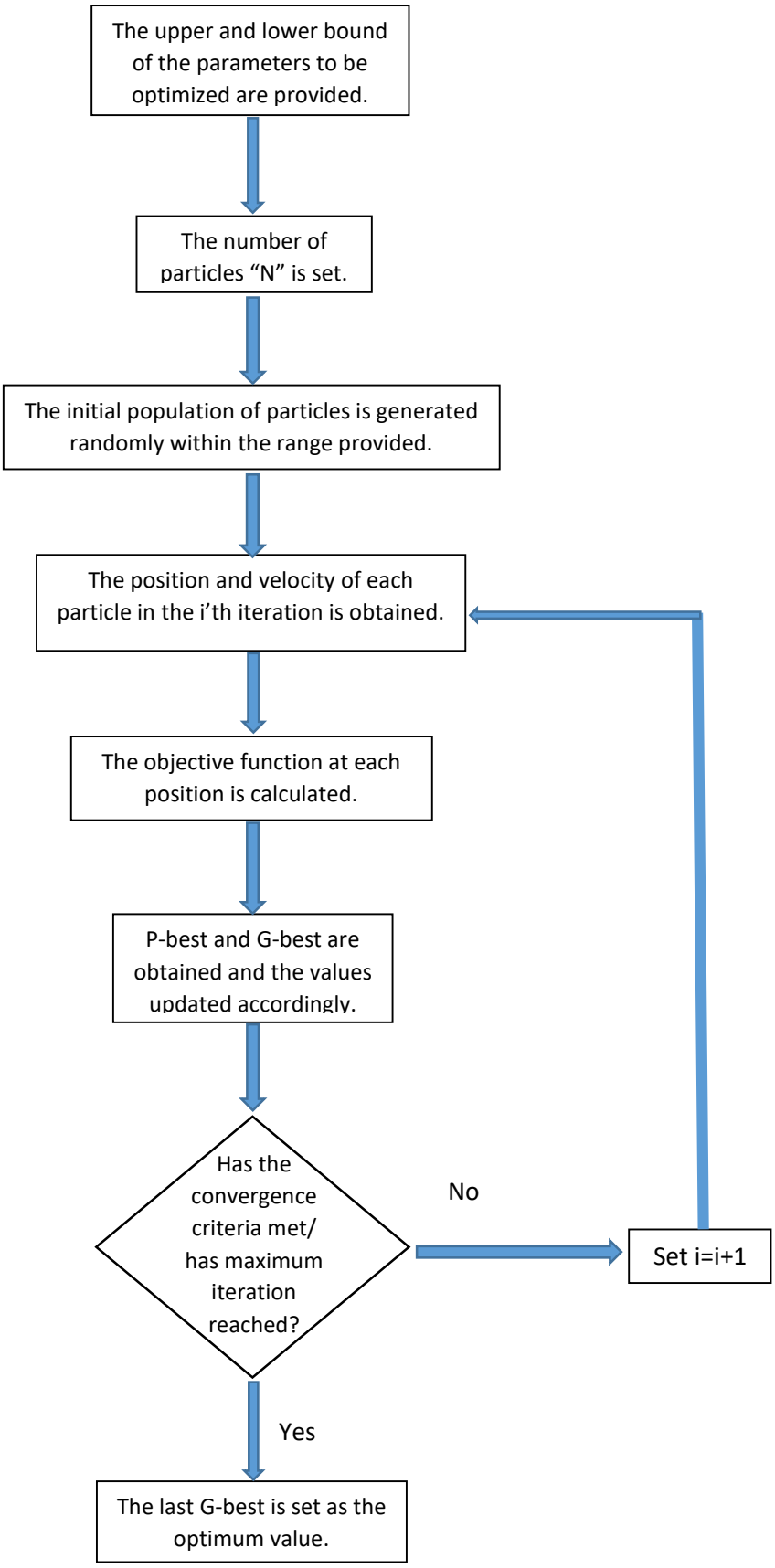

Fig. 3.4. Algorithm for Multi-objective Particle Swarm Optimization

CHAPTER 4

STUDY ON THE EFFECT OF PROCESS PARAMETERS ON SURFACE ROUGHNESS AND HEAT AFFECTED ZONE (HAZ) DURING MARKING ON ALUMINIUM WORK-PIECE

4.1. Experimental Planning

i. Pure Aluminium sheet has been taken for marking using Diode Pump Fiber Laser marking machine that emits at 1064 nm wavelength with a pulse duration of 120ns.

ii. The parameters chosen for the experimentation are Power, Scanning speed and frequency. Values of other parameters i.e. duty cycle, fill spacing, no of passes are kept fixed.

iii. Table 4.1.below shows the range of values taken for each parameters.

Table 4.1. Range of values set for each parameter.

Sl no.	Parameter	Value
1	Duty cycle	99%
2	No of pass	1
3	Fill spacing	10um
3	Frequency	50-110 kHz
4	Power	70%- 90%
5	Scanning speed	4-8mm/s

iv. Using the range of values for the parameters under investigation, single factor experiment is performed taking frequency as the parameter under investigation to check its significance on the process responses i.e. surface roughness and heat affected zone. 4 levels of frequency have been taken keeping values of Power and Scanning speed fixed at 90% of average power and 4mm/s respectively as shown in Table 4.2.

Table 4.2. Single factor experimental values (varying frequency)

Parameter	Value
Power (% of 50 W)	90
Scanning speed (mm/s)	4
Frequency (kHz)	50, 70, 90, 110

Table 4.3.shows the levels of values chosen for frequency.

Table 4.3. Levels chosen for frequency.

Parameter	**Level 1**	**Level 2**	**Level 3**	**Level 4**
Frequency	50	70	90	110

v. Then after Full Factorial format has been constructed using General Full Factorial design taking 2 factors 3 levels for Power and scanning speed keeping frequency fixed as shown in Table 4.4.

Table 4.4. Full factorial experimental values (fixed frequency)

Parameter	Values
Frequency	50 kHz
Power (% of 50W)	90%,80%,70%
Scanning speed (mm/s)	4,6,8

Table 4.5.shows the levels of parameters chosen for Power and scanning speed.

Table 4.5. Levels chosen for Power and Scanning speed.

Parameter	Level 1	Level 2	Level 3
Power (% of 50W)	90%	80%	70%
Scanning speed	4	6	8

vi. Table 4.6 below shows the 9 parametric combinations obtained from full factorial design using MINITAB.

Table 4.6. Parametric combinations of Power and Scanning speed.

No of experiment	**Power (%)**	**Power (P) (W)**	**Scanning speed (Ss) (mm/s)**
1	90	45	6
2	90	45	4
3	70	35	8
4	70	35	4
5	90	45	8
6	80	40	4
7	80	40	8

8	70	35	6
9	80	40	6

vii. Using the above combinations a total of 13 square figures of 2*2 mm² each is marked on the surface of Aluminium as shown in Fig. 4.1 below. This is facilitated by the development of CNC code which is uploaded into the software and run accordingly.

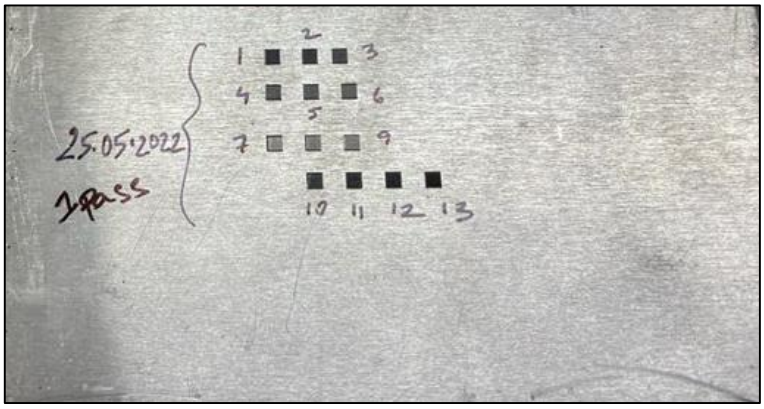

Fig. 4.1. Laser marked Aluminium sample comprising a total of 13 square features.

viii. After the experiment, samples are analysed under the optical microscope OLYMPUS STM 6 for HAZ measurement at a magnification of 5X and the surface roughness is measured using the surface roughness tester.

Fig. 4.2. OLYMPUS STM6 Optical microscope

Procedure for operating OLYMPUS STM6 optical microscope.

i. The microscope is connected to the main power supply and is turned on.
ii. The PC that is connected to the microscope is turned on.
iii. The sample is placed under the lens. The magnification is adjusted using the Z-axis movement of the microscope. The X and Y axis movement is facilitated by rotating the wheel present on the worktable.
iv. The clarity is checked on the monitor as well.
v. The measurement of heat affected zone is then done using the necessary tools available on the software.
vi. The measured values along with the picture of the sample is captured using the "Burn to image" feature available on the software.

4.2. Experimental Results

The results obtained from the single factor experiment is shown below in Table 4.7 and the image observed under the optical microscope is shown in Fig.4.3.

Table 4.7. Experimental results with varying pulse frequency

No of experiments	Power (P) %	Power (P) W	Scanning speed (Ss) mm/s	Pulse frequency (f) kHz	Surface roughness (Ra) um	Heat affected zone (HAZ) um
1	90	45	4	50	5.286	85.56
2	90	45	4	70	4.998	82.92
3	90	45	4	90	5.154	67.85
4	90	45	4	110	4.392	49.34

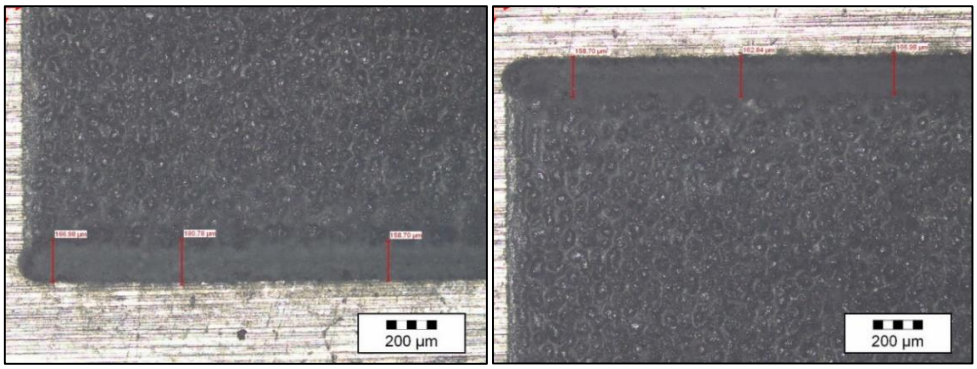

Fig.4.3. Laser marked Aluminium sample obtained from single factor experiment (varying frequency) observed under OYMPUS STM 6 optical microscope for HAZ measurement.

Table 4.8 below shows the values of the process criteria i.e. Heat affected zone (HAZ) and Surface Roughness obtained for each data sets for 9 different factorial experiments.

Table 4.8. Experimental results with fixed pulse frequency of 50 kHz.

No of experiments	Power (P) %	Power (P) W	Scanning speed (Ss) mm/s	Surface roughness (Ra) um	Heat affected zone (HAZ) um
1	90	45	6	2.638	94.83
2	90	45	4	5.277	95.22
3	70	35	8	1.17	78.55
4	70	35	4	3.194	88.46
5	90	45	8	0.584	92.92
6	80	40	4	3.813	90.21
7	80	40	8	0.992	84.52
8	70	35	6	2.525	83.03
9	80	40	6	3.381	85.91

Fig.4.4.shows some of the laser marked images of Aluminium observed under the optical microscope for HAZ measurement.

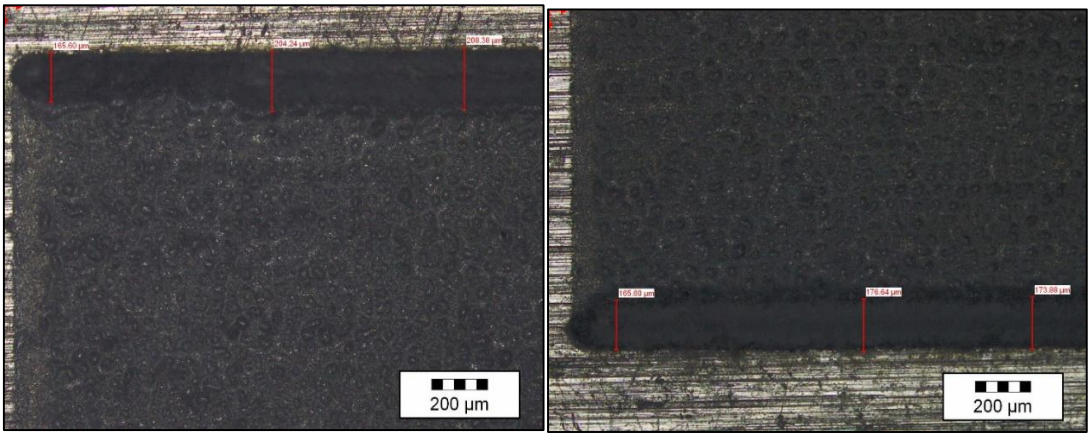

Fig.4.4.Laser marked Aluminium sample observed under OYMPUS STM 6 optical microscope for HAZ measurement.

4.3. Study of The Effect of Laser Power and Scanning Speed on Heat Affected Zone and Surface Roughness.

The relationship between the process parameters and the process responses is studied using scatter plots. The plots taken for investigation are as follows:

i. Frequency v/s Surface roughness
ii. Frequency v/s HAZ
iii. Power v/s HAZ on different scanning speed
iv. Scanning speed v/s HAZ on different Power
v. Power v/s Ra on different scanning speed
vi. Scanning speed v/s Ra on different Power

All the above relationships are represented in Fig. 4.5 (a-b) Fig.4.6. (a-d) and below.

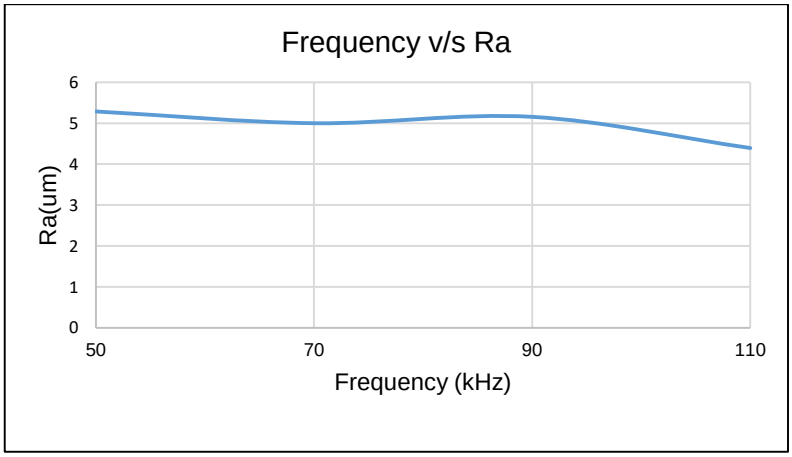

a)

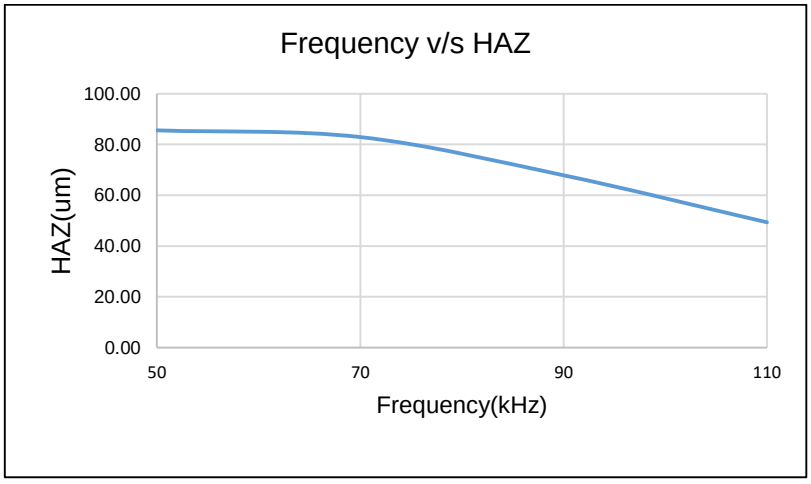

b)

Fig. 4.5. Effect of frequency on Surface roughness (Ra) and Heat affected zone (HAZ)

In Fig.4.5 (a) the effect of frequency on Ra has been shown. It can be observed that with the increase in frequency Ra almost remains constant or decreases since increase in frequency is accompanied by decrease in average power and hence the amount of material removal decreases which leads to a little or no change in Ra.

In Fig.4.5 (b) it can be seen that HAZ decreases with increasing frequency reason being similar to that explained above .Low power will cause less thermal effects to take place on the material thereby reducing HAZ.

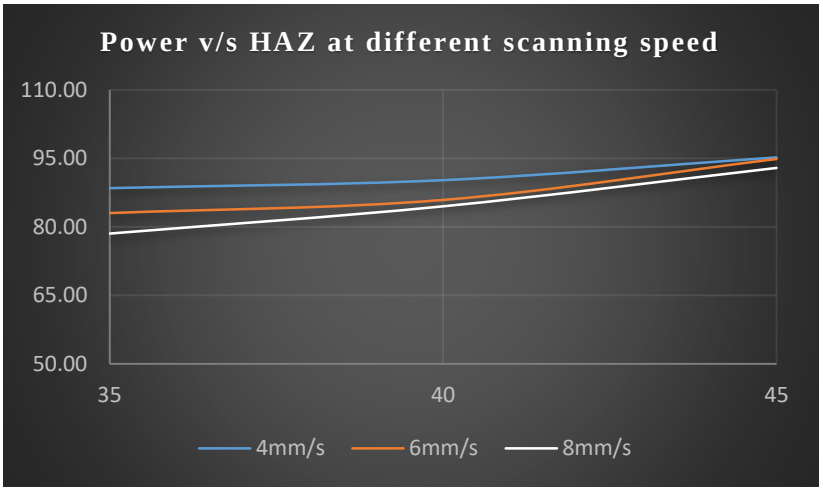

a)

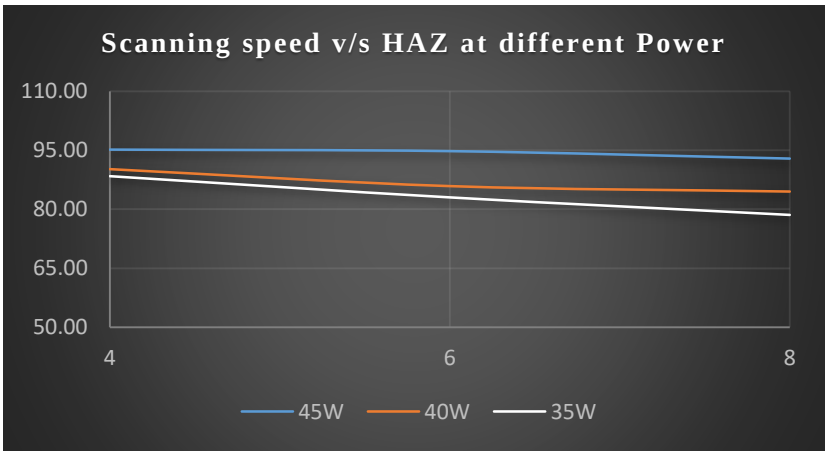

b)

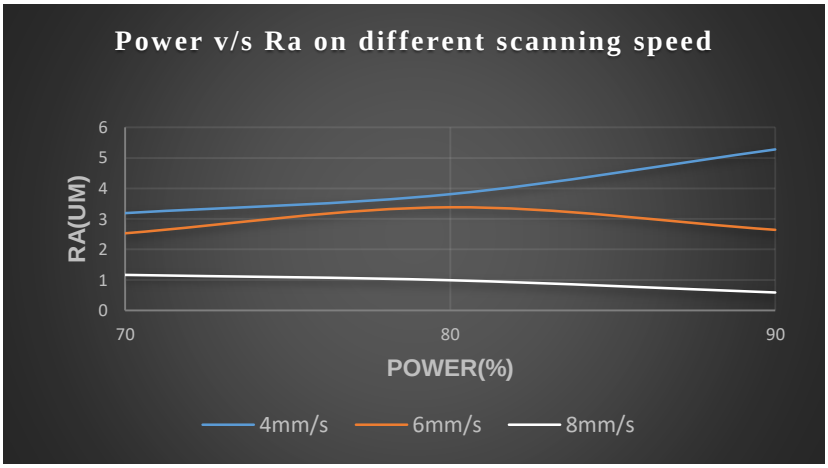

c)

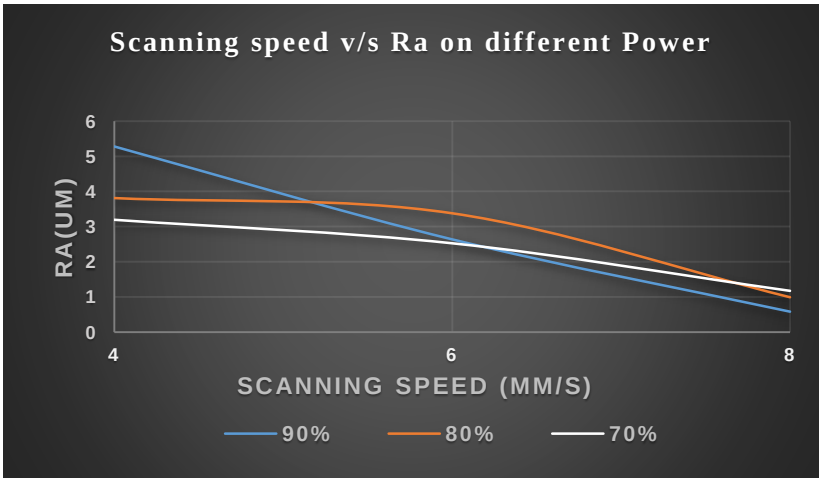

d)

Fig.4.6 (a-d). Effect of Power and Scanning speed on HAZ and Surface roughness (Ra).

In Fig.4.6 (a) above, the relationship between laser power and heat affected zone (HAZ) on different scanning speed has been depicted. The plot shows that with the increase in laser power the HAZ increases gradually for each scanning speed. The reason behind this being more the power, more is the energy available for removing the material. However, in the given time frame the energy being in excess will start getting transferred in the surrounding areas due to conduction which will lead to unwanted heating and melting of additional areas that can later on lead to formation of re-solidified layers thereby increasing the heat affected zone.

In Fig. 4.6 (b), the relationship between scanning speed and HAZ on different power has been represented. It can be seen that with the increase in scanning speed, the HAZ takes almost a constant or a gradual negative slope in this case. The almost constant behaviour shows that in this case scanning speed does not have a very significant effect on HAZ. However the slight

negative slope seen above can be explained by the fact that on increasing the scanning speed the interaction time between the laser and the irradiated area decreases thereby providing insufficient energy for the material removal. Hence the question of heat getting transferred to the surrounding areas get ruled out giving lesser or no HAZ. This behaviour can be observed in case of [33] wherein laser marking on stainless steel 304 have been done and the effect of scanning speed on mark depth and width has been studied.

In Fig. 4.6 (c), the effect of Power on Surface roughness (Ra) has been depicted. It can be observed that the behaviour of laser power on Ra is slightly different for different scanning speeds. For scanning speed of 4mm/s, with the increase in power the Ra increases reason being more amount of interaction between the surface and laser leading to more thermal effects on the material. On increasing the scanning speed to 6mm/s similar behaviour is observed but up to a certain power value. On increasing the power further causes an almost constant or a slight decrease in Ra. The reason could be that on further increasing the power the energy is so much that it leads to complete vaporization of the irradiated zone leading to a smooth surface. Coming to a scanning speed of 8mm/s there is an almost no change in Ra. In this case there is almost no change or a slight decrease in Ra reason being since the speed is so high, there is very less interaction between the material and the laser that almost no or only a small amount of material is undergoing thermal effects which on vaporisation leads to smoothening of the surface decreasing Ra.

In Fig. 4.6 (d), the relationship between scanning speed and surface roughness on different laser power has been given. It can be inferred from the plot that with the increase in scanning speed for each values of laser power, the surface roughness decreases. The reason for this can be, at lower scanning speeds, the interaction time between the material and the laser being more will lead to more amount of material removal wherein the proportion of melting taking place is more which contributes to a rougher surface due to solidification of this non- ejected melt pool leading to formation of sharp peaks and valleys. Now as the scanning speed increases the interaction time between the material and the laser is insufficient to cause melting of the irradiated zone and only causing slight heating causing removal of very small particles of the irradiated zone thereby decreasing the surface roughness. The similar effect of scanning speed can be observed in [25] & [43] in which marking on aluminium alloy and Titanium has been done respectively.

4.4. Analysis of Variance for Surface roughness and Heat affected zone (Ra and HAZ)

Regression analysis also known as predictive modelling technique is a statistical modelling technique which helps understand how one variable is related to the other and helps sort out variables that matter the most. It helps predict the value of a dependent variable based on one or more independent variables.

Fitting a model is done to choose a statistical model that helps predict values of the responses as close as possible to the observed values. In the present scenario Fit Regression Model is used. This gives a relation between a set of continuous predictors and responses using the least squares method which is a method of finding the best-fitting curve for a set of data points by reducing the sum of squares.

Here the process responses or the dependent variables chosen are surface roughness 'Ra' and heat affected zone 'HAZ'. Using MINITAB the experimental results obtained for a set of combinations derived from Full factorial DOE is used and mathematical model for predicting the values of the process responses are obtained. ANOVA (analysis of variance) test is done to check the efficacy of the model. While checking, it is ensured that the P-value, which shows the probability of the observed difference that could have occurred by chance, is less than or equal to 0.05 which proves the significance of the mathematical model thus obtained.

The ANOVA table for the above regression model for surface roughness and HAZ is given below in Table 4.9 and Table 4.10 respectively.

Table 4.9. ANOVA for Surface roughness (Ra).

Source	DF	Adj SS	Adj MS	F- Value	P- Value	Remarks
Regression	3	17.3751	5.7917	31.34	0.001	Significant
Power	1	2.1324	2.1324	11.54	0.019	Significant
Scanning speed	1	0.8691	0.8691	4.70	0.082	Insignificant
Power*Scanning speed	1	1.7809	1.7809	9.64	0.027	Significant
Error	5	0.9239	0.1848			
Total	8	18.2990				

MODEL SUMMARY			
S	R-sq	R-sq(adj)	R-sq(pred)
0.429854	94.95%	91.92%	87.92%

From Table 4.11. we can infer that apart from one parameter i.e. scanning speed, all the other parameters are significant and the model R-squared value of 94.95 % shows that the model fits the data well.

The empirical model thus obtained for Ra is given in equation (4.1) below.

$$\mathbf{Ra} = -\mathbf{10.77} + \mathbf{0.454\,P} + \mathbf{1.874\,Ss} - \mathbf{0.0667\,P} * \mathbf{Ss} \quad \text{Eq. (4.1)}$$

Table 4.10. ANOVA for Heat affected zone (HAZ)

Source	DF	Adj SS	Adj MS	F-Value	P-Value	Remarks
Regression	5	256.617	51.3235	90.23	0.002	Significant
Power	1	7.610	7.6098	13.38	0.035	Significant
Scanning speed	1	12.348	12.3483	21.71	0.019	Significant
Power*Power	1	7.648	7.6475	13.45	0.035	Significant
Scanning speed*Scanning speed	1	0.305	0.3049	0.54	0.517	Insignificant

MODEL SUMMARY			
S	R-sq	R-sq(adj)	R-sq(pred)
0.754185	99.34%	98.24%	94.05%

From Table 4.10 we can observe that all the parameters are significant except one i.e. scanning speed * scanning speed and the model R-squared value of 99.34 % shows that the model perfectly fits the data.

The empirical model thus obtained for HAZ is given in equation (4.2) below.

$$\boldsymbol{HAZ} = \mathbf{226.0} - \mathbf{6.30}\,\boldsymbol{P} - \mathbf{10.27}\,\boldsymbol{Ss} + \mathbf{0.0782}\,\boldsymbol{P} * \boldsymbol{P} + \mathbf{0.098}\,\boldsymbol{Ss} * \boldsymbol{Ss} + \mathbf{0.1902}\,\boldsymbol{P} * \boldsymbol{Ss} \quad \text{Eq. (4.2)}$$

In equations (3) and (4) **'P'** and **'Ss'** are the independent variables / un-coded values of Power and Scanning speed where,

$\mathbf{35 \leq P \leq 45}$ **(W) and** $\mathbf{4 \leq Ss \leq 8}$ **(mm/s)**

4.5. Optimisation using Multi-Objective Particle Swarm Optimization Technique (MOPSO)

For MOPSO the parameters taken for optimization are Power and Scanning speed. The upper and lower limit are taken from Table 8.in which $\mathbf{35 \leq P \leq 45}$ **and** $\mathbf{4 \leq Ss \leq 8.}$

Taking into consideration one of the industrial applications of laser marking i.e. laser marking QR code for product identification, the objective of the present research is to maximize Ra and minimize HAZ. Studies have found that maximizing Ra improves the contrast of the QR code marked, which is one of the important factors affecting the grade of the code thus obtained [25]. On the other hand heat affected zone is something that increases the print growth of the mark which renders the readability of the code. Hence a mark with minimum/no HAZ outside of the working area is always preferred.

Therefore from equations (3) and (4) objective function is stated as below:

Maximize Ra= -10.77 + 0.454 P + 1.874 Ss - 0.0667 P*Ss

Minimize HAZ=226.0 - 6.30 P - 10.27 Ss + 0.0782 P*P+ 0.098 Ss*Ss + 0.1902 P*Ss

The possible combinations of parameters thus obtained from MOPSO which gives the global optimum values of the two process responses is given below in Table 4.11.

Table 4.11. Combinations of parameters giving global optimum values of process responses.

Sl no.	Power (P) W	Scanning speed (Ss) mm/s	Surface roughness (Ra) um	Heat affected zone (HAZ) um
1	35.0000	8.0000	1.4360	78.6630
2	35.0495	7.9999	1.4321	78.6978
3	35.1185	8.0000	1.4266	78.7465
4	35.1795	7.9999	1.4217	78.7905
5	35.2752	8.0000	1.4141	78.8603
6	35.3370	7.9999	1.4092	78.9064
7	35.4232	8.0000	1.4023	78.9715
8	35.5243	8.0000	1.3943	79.0493
9	35.5865	8.0000	1.3893	79.0979
10	35.6528	8.0000	1.3840	79.1504

11	35.7216	7.9992	1.3790	79.2072
12	35.7510	8.0000	1.3762	79.2295
13	35.8054	7.9999	1.3719	79.2742
14	35.8562	7.9999	1.3679	79.3160
15	35.9410	8.0000	1.3611	79.3868
16	35.9684	8.0000	1.3589	79.4100
17	36.0177	8.0000	1.3550	79.4519
18	36.0828	7.9999	1.3498	79.5080
19	36.1418	7.9999	1.3451	79.5594
20	36.2667	8.0000	1.3352	79.6696
21	36.3124	8.0000	1.3315	79.7106
22	36.3750	8.0000	1.3266	79.7673
23	36.4694	7.9999	1.3191	79.8541
24	36.5185	8.0000	1.3151	79.8996
25	36.6190	8.0000	1.3071	79.9942
26	36.6686	7.9999	1.3032	80.0415
27	36.7214	7.9999	1.2990	80.0923
28	36.7793	7.9998	1.2945	80.1486
29	36.8434	7.9998	1.2894	80.2114
30	36.9154	8.0000	1.2835	80.2823
31	36.9668	8.0000	1.2794	80.3336
32	37.0468	8.0000	1.2731	80.4145
33	37.0889	8.0000	1.2697	80.4573
34	37.1479	7.9999	1.2651	80.5181
35	37.2614	8.0000	1.2560	80.6360
36	37.3147	8.0000	1.2518	80.6921
37	37.3549	7.9987	1.2494	80.7368
38	37.4057	7.9997	1.2447	80.7894
39	37.4570	8.0000	1.2404	80.8441
40	37.5361	7.9996	1.2344	80.9306

Table 4.11 above is a list of combinations of parameters that provides us global optimum values of Ra and HAZ obtained through MOPSO technique. As mentioned earlier since our priority is to obtain marks with maximum Ra and minimum HAZ, from the table above our objective is fulfilled when Power of 35W with a scanning speed of 8mm/s is used. The maximum value of Ra thus obtained using this combination is 1.4360um and minimum HAZ obtained is 78.6630um.

The Pareto Front shown below obtained from MOPSO shows the convergence and even distribution of the particles giving us the final global optimum solutions which evaluates the quality of the final solution obtained for Surface roughness(Ra) and Heat affected zone (HAZ).

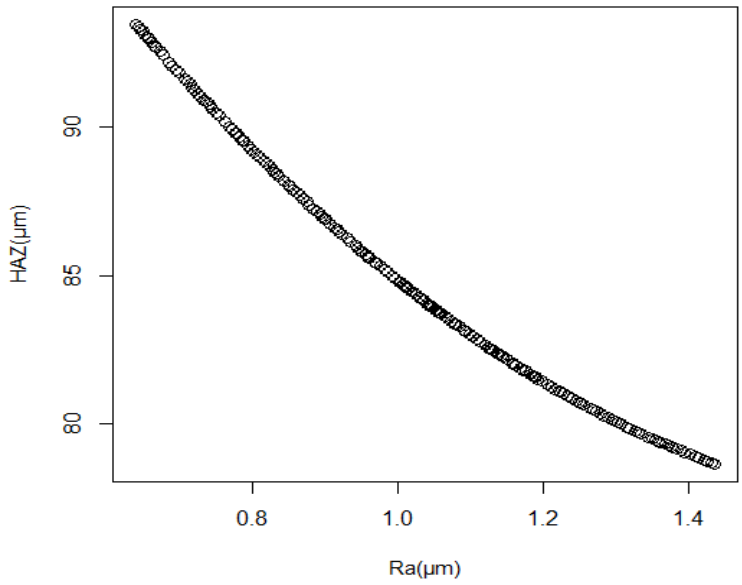

Fig. 4.7 Pareto Front of heat affected zone (HAZ) v/s surface roughness (Ra) obtained from MOPSO.

From the graph it can be observed that with the increase in Ra, HAZ decreases and for Ra lying in the range between 0.6um – 1um the decline in HAZ is quite rapid after which the decline is slightly gradual. For Ra lying in the range between 1.2um – 1.4um, minimum HAZ in the range of 82um- 76um (approx.) can be obtained.

CHAPTER 5-
STUDY ON THE EFFECT OF PROCESS PARAMETERS ON SURFACE ROUGHNESS AND HEAT AFFECTED ZONE (HAZ) DURING MARKING ON BERYLLIUM COPPER WORK-PIECE

5.1. Experimental Planning

1. Beryllium Copper sheet has been taken for marking using Diode Pump Fiber Laser marking machine that emits at 1064 nm wavelength with a pulse duration of 120ns.
2. The parameters chosen for the investigation are Power and Scanning speed. Values of other parameters i.e. duty cycle, frequency, fill spacing, no of passes are kept fixed.
3. Through literature surveys and trial experiments the range of values for each parameters is chosen according to Table 5.1.below.

Table 5.1. Values set for each parameter.

Sl no.	Parameter	Value
1	Duty cycle	99%
2	No of pass	1
3	Fill spacing	10um
3	Frequency	50 kHz
4	Power	30%- 50%
5	Scanning speed	4-8mm/s

4. Using the range of values for the 2 parameters under investigation, Full factorial DOE is constructed using 2 factors 3 levels for Power and scanning speed.

   Table 5.2.shows the levels of power and scanning speed chosen for the marking experiment.

Table 5.2. Levels of each parameter chosen.

Parameter	Level 1	Level 2	Level 3
Power (% of 50W)	30%	40%	50%
Scanning speed	4	6	8

5. Using the general full factorial design taking the above levels of parameters, the parametric combinations for the experiment is obtained using MINITAB and is shown below in Table 5.3.

Table 5.3. Parametric combinations of Power and Scanning speed.

No of experiment	Power (P) %	Power (P) (W)	Scanning speed (Ss) mm/s
1	50	25	4
2	40	20	4
3	30	15	4
4	50	25	8
5	50	25	6
6	30	15	8
7	40	20	8
8	30	15	6
9	40	20	6

6. Using the above combinations a total of 9 square features of 2*2 mm^2 each is marked on the surface of beryllium copper as shown in Fig. 5.2 below. This is facilitated by the development of CNC code which is uploaded into the software and run accordingly.

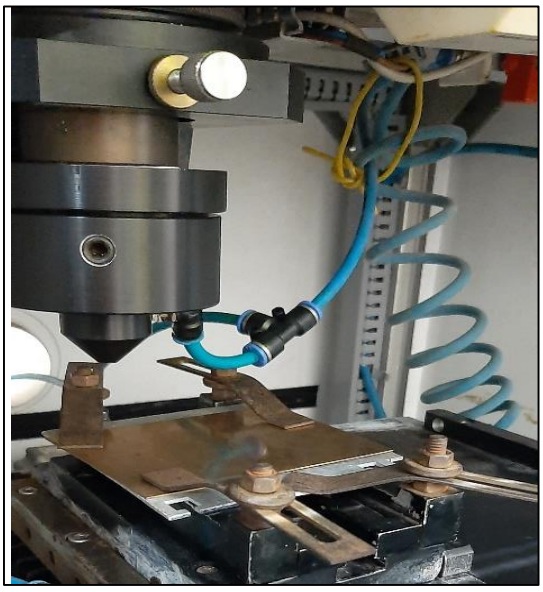

Fig 5.1. Laser marking operation on Beryllium Copper sheet.

Fig. 5.2. Laser marked Beryllium Copper sample comprising a total of 9 squares.

7. After the experiment, samples are analysed under the optical microscope ZEISS STEMI 508 for HAZ measurement at a magnification of 4X and the surface roughness is measured using the surface roughness tester.

Fig 5.3. ZEISS STEMI 508 optical microscope used for HAZ measurement.

Procedure for operating the optical microscope ZEISS STEMI 508 for heat affected zone measurement

i. The microscope is connected to the main power supply and to the PC which contains the software named SCOPEIMAGE which is used to do all the necessary measurements using the microscope. Measurements are obtained in microns.

ii. The power button of the microscope is switched on.

iii. The laser marked sample is placed under the lens.

iv. The microscope magnification is adjusted according to our convenience depending on the clarity of the required features. This is done by rotating the Z-axis movement knob present in the microscope.

v. Clarity on the monitor is also checked before finalizing the magnification since that will help obtain accurate measurement. The ZEISS STEMI 508 microscope has magnifications ranging from 2X to 5X.

vi. After the magnification on the microscope is finalized, the magnification level on the software is selected accordingly before taking the measurement of HAZ.

vii. Finally using the tools available on the software the required measurement of HAZ is taken and recorded.

5.2. Experimental Results

Table 5.4.below shows the values of the process criteria i.e. Heat affected zone (HAZ) and Surface Roughness (Ra) obtained for each data sets for 9 different full factorial experiments. Fig. 5.4.shows some of the laser marked images observed under the optical microscope for HAZ measurement.

Table 5.4. Experimental results of heat affected zone (HAZ) and Surface roughness (Ra) of Beryllium copper.

No of experiments	Power (P) %	Power (P) W	Scanning speed (Ss) mm/s	Heat affected zone (HAZ) (um)	Surface roughness (Ra) um
1	50	25	4	103.230	0.440
2	40	20	4	87.732	0.310
3	30	15	4	70.330	0.201
7	50	25	8	99.050	0.226
4	50	25	6	101.611	0.260
9	30	15	8	74.679	0.209
8	40	20	8	85.693	0.225
6	30	15	6	75.472	0.200
5	40	20	6	85.000	0.230

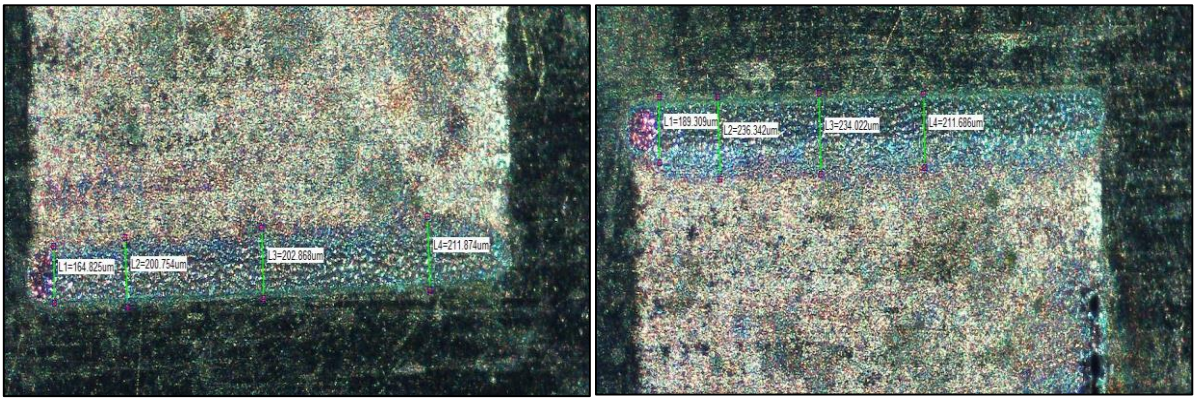

Fig 5.4. Laser marked Beryllium copper sample observed under optical microscope STEMI 508 for HAZ measurement.

5.3. Study of The Effect of Laser Power and Scanning Speed o Heat Affected Zone and Surface Roughness of Copper.

The relationship between the process parameters and the process responses is studied using the scatter plots. The plots taken for investigation are as follows:

i. Power v/s HAZ on different scanning speed
ii. Scanning speed v/s HAZ on different Power
iii. Power v/s Ra on different scanning speed
iv. Scanning speed v/s Ra on different Power

All the above plots are represented in Figure 5.5 (a-d) below.

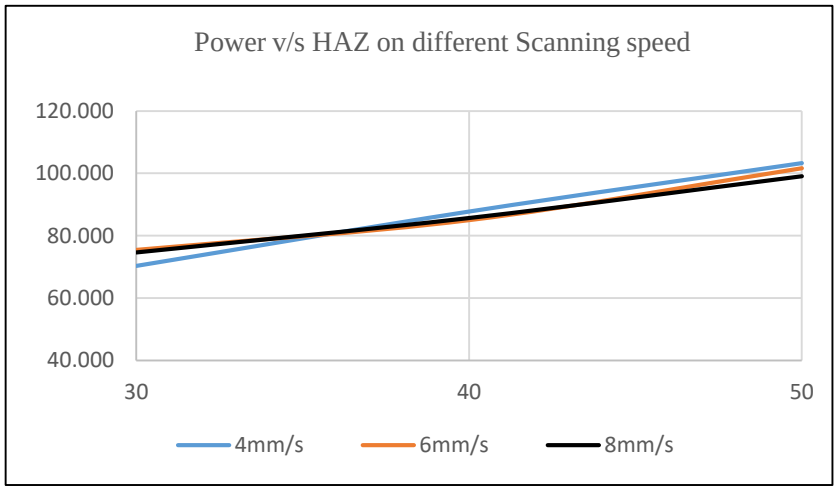

a)

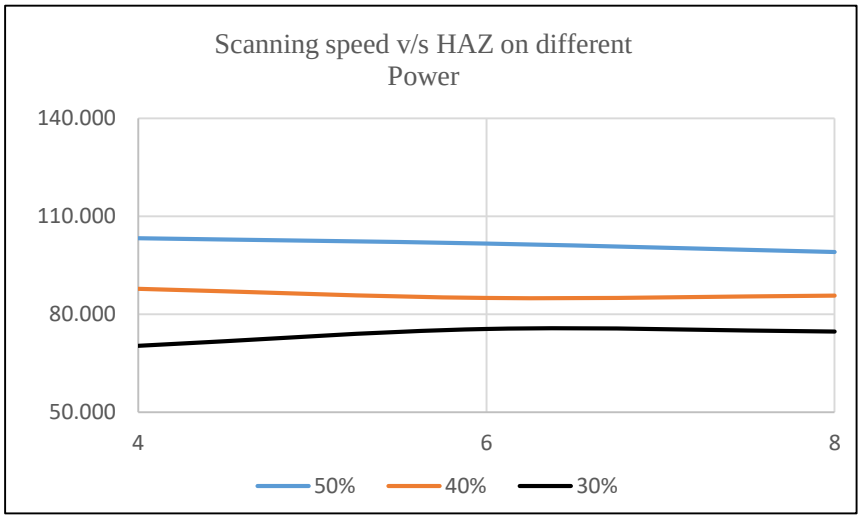

b)

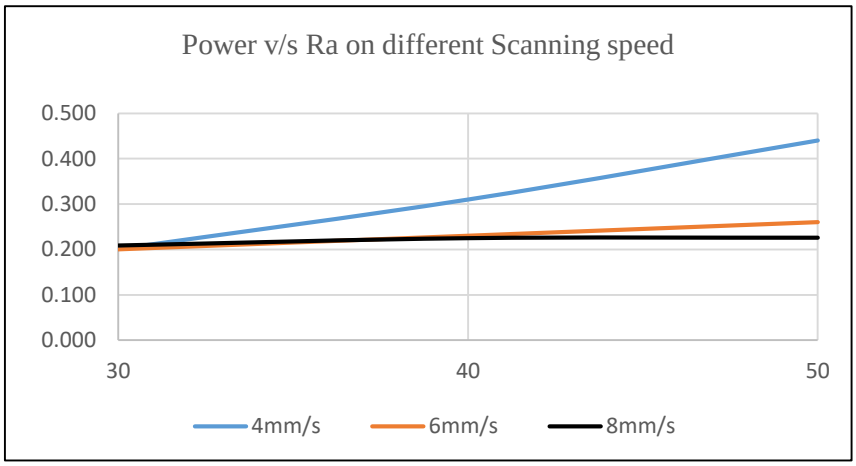

(c)

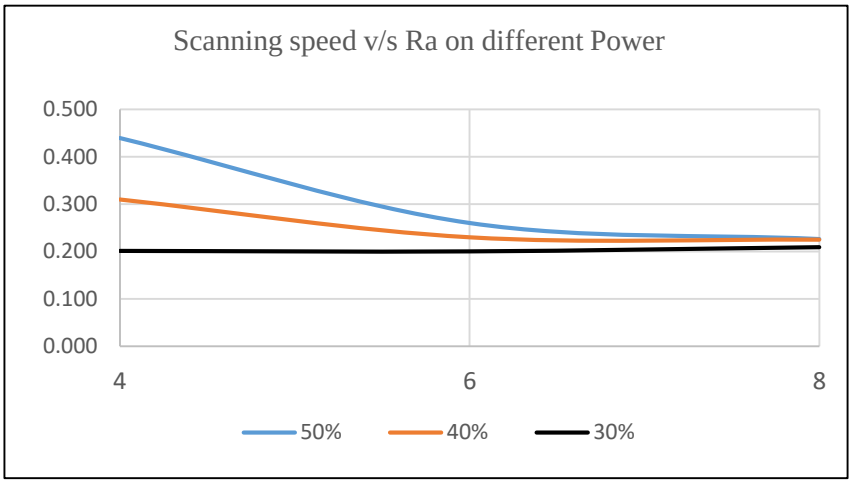

(d)

Fig 5.5. (a- d). Effect of Laser Power and Scanning speed on HAZ and Surface roughness of Copper.

In Fig 5.5 (a), the relationship between laser Power and Heat affected zone (HAZ) has been depicted. It can be observed from the plot that with the increase in power, heat affected zone increases for all values of scanning speed. The reason being more the Power, more is the energy available for material removal and the excess energy gets transferred to the surrounding areas causing thermal effects away from the working zone. Also it can be seen that there is a very minor change in HAZ for different scanning speeds.

In Fig 5.5 (b), the effect of scanning speed on HAZ has been shown. It can be observed that with the increase in scanning speed, there is little or no effect on HAZ. This shows that in the particular case of laser marking on Copper, scanning speed does not have a significant effect on the development of heat affected zone reason being the power used is already so less that on increasing the scanning speed no such major changes are observed.

In Fig 5.5 (c), relationship between power and surface roughness (Ra) has been depicted. The graph shows that on increasing the laser power for a scanning speed of 4mm/s Ra increases reason being more the Power more the energy available for material removal and the scanning speed being less increases the interaction time between the material and the work-piece causing formation of additional melt pool which doesn't get ejected leading to the formation of sharp peaks and valleys on solidification. Upon increasing the scanning speed the effect on Ra w.r.t. power becomes negligible reason being as stated above in Fig 5.5(b).

In Fig 5.5 (d), effect of scanning speed on Ra has been shown. With the increase in scanning speed for a higher laser power of 50% and 40%, Ra decreases up-to a certain point and after that becomes almost constant and for a power of 40% there is almost no change in Ra. On increasing the scanning speed, the interaction time between the surface and the laser decreases causing removal of very small particles reducing Ra and on further increasing the scanning speed there is almost no thermal effects taking place causing no change in Ra.

5.4. Analysis of Variance for Surface roughness and Heat affected zone (HAZ)

Here the process responses or the dependent variables chosen are surface roughness 'Ra' and heat affected zone 'HAZ'. Using MINITAB the experimental results obtained for a set of combinations derived from Taguchi DOE is used and mathematical model for predicting the values of the process responses are obtained. ANOVA (analysis of variance) test is done to check the efficacy of the model. While checking, it is ensured that the P-value, which shows

the probability of the observed difference that could have occurred by chance, is less or equal to than 0.05 which proves the significance of the mathematical model thus obtained.

The ANOVA table for the regression model for Ra and HAZ is given below in Table 5.5 and Table 5.6 respectively.

Table 5.5. ANOVA for Surface Roughness (Ra).

Source	DF	Adj SS	Adj MS	F-Value	P-Value	Remarks
Regression	5	0.047583	0.009517	257.21	0.000	Significant
Power	1	0.004633	0.004633	125.22	0.002	Significant
Scanning speed	1	0.001267	0.001267	34.24	0.010	Significant
Scanning speed*Scanning speed	1	0.000760	0.000760	20.55	0.020	Significant
Power*Scanning speed	1	0.002471	0.002471	66.79	0.004	Significant
Power*Scanning speed*Scanning speed	1	0.001541	0.001541	41.66	0.008	Significant
Error	3	0.000111	0.000037			
Total	8	0.047694				

MODEL SUMMARY			
S	R-sq	R-sq(adj)	R-sq(pred)
0.0060828	99.77%	99.38%	96.86%

From Table 5.5 it is observed that all the parameters are statistically significant and from the model summary an R-squared value of 99.77% shows us that the model perfectly fits the data well. The regression equation (5.1) thus obtained for surface roughness (Ra) is given below.

$$\boldsymbol{Ra = -1.288 + 0.10050\,P + 0.3792\,Ss - 0.02437\,Ss*Ss - 0.02595\,P*Ss + 0.001700\,P*Ss*Ss} \quad \text{Eq. (5.1)}$$

Table 5.6.shows the ANOVA for heat affected zone (HAZ).

Table 5.6. ANOVA for Heat affected zone.

Source	DF	Adj SS	Adj MS	F-Value	P-Value	Remarks
Regression	3	1178.28	392.760	155.62	0.000	Significant
Power	1	170.50	170.496	67.56	0.000	Significant
Scanning speed	1	16.21	16.208	6.42	0.052	Insignificant

Power*Scanning speed	1	18.19	18.188	7.21	0.044	Significant
Error	5	12.62	2.524			
Total	8	1190.90				

MODEL SUMMARY			
S	R-sq	R-sq.(adj)	R-sq(pred)
1.58864	98.94%	98.30%	97.23%

From Table 5.6, it can be observed that all the combinations except scanning speed are significant. This goes well with the graph obtained in Fig 5.4(b) which shows that scanning speed doesn't have a major effect on HAZ. The model summary shows that R-square of 98.94% is achieved which indicates that the model fits the data well.

The mathematical model thus obtained for HAZ is given below in equation (5.2).

$$\boldsymbol{HAZ = 6.7 + 4.060\,P + 4.11\,Ss - 0.2132\,P * Ss} \quad \text{Eq. (5.2)}$$

In equation (5) and equation (6), 'P' and 'Ss' are the independent values of Power (W) and Scanning speed (Ss) respectively and

$$\boldsymbol{15 \leq P \leq 25\ (W) and\ 4 \leq Ss \leq 8\ (\frac{mm}{s})}$$

5.5. Optimization using Multi- Objective Particle Swarm Optimization Technique (MOPSO)

For MOPSO the parameters taken for optimization are Power and Scanning speed. The upper and lower limit are taken from table 8.in which $\boldsymbol{15 \leq P \leq 25}$ **and** $\boldsymbol{4 \leq Ss \leq 8.}$

Taking into consideration the similar industrial application of laser marking i.e. laser marking QR code for product identification, the objective of the present research is to maximize Ra and minimize HAZ. Studies have found that maximizing Ra improves the contrast of the QR code marked, which is one of the important factors affecting the grade of the code thus obtained [25]. On the other hand heat affected zone is something that increases the print growth of the mark which renders the readability of the code. Hence a mark with minimum/no HAZ outside of the working area is always preferred.

Therefore from equation 5 and equation 6, the objective of the present research is stated below as:

Maximize $Ra = -1.288 + 0.10050\,P + 0.3792\,Ss - 0.02437\,Ss * Ss - 0.02595\,P * Ss + 0.001700\,P * Ss * Ss$

Minimize $HAZ = 6.7 + 4.060\,P + 4.11\,Ss - 0.2132\,P * Ss$

Table 5.7 are the possible combinations of the chosen parameters i.e. Power and Scanning speed that helps obtain global optimum values of the process responses i.e. Ra and HAZ using MOPSO technique.

Table 5.7. Global optimum results using MOPSO.

Sl.no	Power (P) W	Scanning speed (Ss) mm/s	Surface roughness (Ra) um	Heat affected zone (HAZ) um
1	15	4	0.197380	71.2480
2	15	4.001501	0.197379	71.2494
3	15	4.002396	0.197378	71.2502
4	15	4.00381	0.197376	71.2515
5	15	4.004586	0.197376	71.2522
6	15	4.006847	0.197373	71.2542
7	15	4.007126	0.197373	71.2545
8	15	4.008386	0.197372	71.2557
9	15	4.010248	0.197370	71.2574
10	15	4.010775	0.197369	71.2578
11	15	4.012068	0.197368	71.2590
12	15	4.013334	0.197367	71.2602
13	15	4.014678	0.197365	71.2614
14	15	4.015496	0.197365	71.2621
15	15	4.016488	0.197364	71.2630
16	15	4.016923	0.197363	71.2634
17	15	4.01762	0.197363	71.2641
18	15	4.018374	0.197362	71.2648
19	15	4.019685	0.197361	71.2660
20	15	4.01985	0.197360	71.2661
21	15.00001	4.020817	0.197360	71.2670
22	15	4.021831	0.197359	71.2679
23	15	4.02323	0.197357	71.2692
24	15	4.024331	0.197356	71.2702
25	15	4.025253	0.197355	71.2710
26	15	4.026193	0.197354	71.2719
27	15	4.026274	0.197354	71.2720
28	15	4.027251	0.197353	71.2729
29	15	4.028718	0.197352	71.2742
30	15	4.031085	0.197350	71.2764

31	15.00002	4.032796	0.197349	71.2780
32	15	4.034238	0.197347	71.2792
33	15	4.035387	0.197346	71.2803
34	15	4.037418	0.197344	71.2821
35	15	4.039344	0.197342	71.2839
36	15	4.040887	0.197341	71.2853
37	15	4.042311	0.197339	71.2866
38	15	4.043169	0.197339	71.2874
39	15	4.044184	0.197338	71.2883
40	15	4.046783	0.197335	71.2907

From Table 5.7 it can be observed that the objective function is satisfied for the parameter combination of Power and Scanning speed as 15W and 4mm/s respectively helping us achieve a maximum surface roughness of 0.1974 um and minimum HAZ of 71.2480um.

Below Pareto graph, Fig 5.6. obtained from Multi-objective Particle swarm optimization shows the relationship between HAZ and Ra.

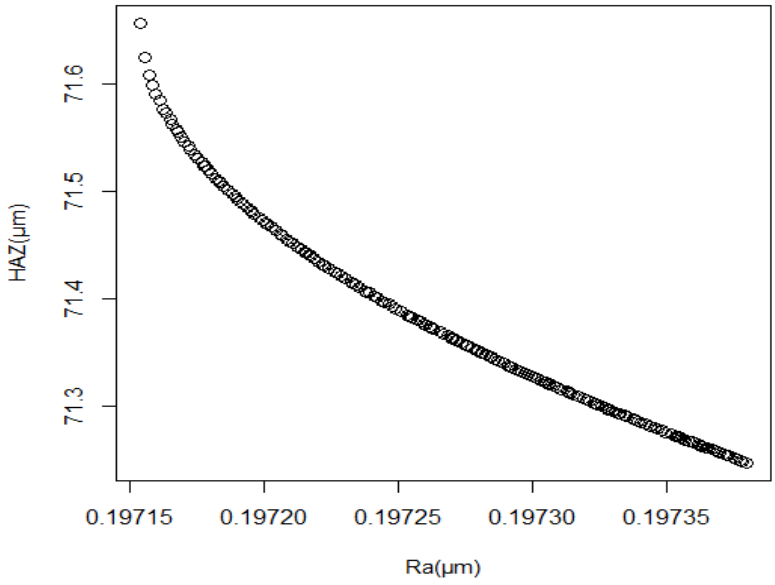

Fig. 5.6. Pareto Front of heat affected zone (HAZ) of v/s surface roughness (Ra) obtained from MOPSO.

From the graph it can be inferred that with the increase in Ra, heat affected zone decreases gradually in the surface roughness range of 0.19715 to 0.19720 um after which the decrease is HAZ gets a bit sharp and for a higher value of Ra, HAZ lying in the range of 71.1um to 71.3 um is obtained.

CHAPTER 6

GENERAL CONCLUSION AND FUTURE SCOPE OF THE WORK

6.1. General Conclusion

In the present research, laser marking process on a light metal i.e. Aluminium and light metal alloy i.e., Beryllium Copper has been investigated using a Multi-Diode Pump Fiber Laser Marking machine. The effect of certain parameters on the surface roughness and heat affected zone has been investigated. Optimization of those parameters using Multi Objective Particle Swarm Optimization (MOPSO) technique has also been carried out.

Within the limitations of the present research, the analysis on the detailed experimental observations, the following general conclusions maybe be drawn.

a) The process of Laser marking has been studied through substantial literature survey.
b) The parameters chosen for the investigation were Power, frequency and scanning speed for Aluminium and Power and scanning speed for Beryllium copper. Other parameters like current, duty cycle, fill spacing, pulse duration, etc. were kept fixed.
c) Through trial experiments, the working range and levels of the process parameters has been identified for the respective materials i.e., Aluminium and Beryllium Copper.
d) Laser direct marking on the two materials has been done by designing the experiment using full factorial DOE.
e) Measurements of surface roughness and heat affected zone were done using surface roughness tester and optical microscope.
f) Effect of laser power, scanning speed and frequency on the responses were studied in case of Aluminium and effect of power and scanning speed were studied in case of Copper using scatter plots and the following conclusions were made.
    1. With the increase in laser power both heat affected zone and surface roughness increased for all values of scanning speed.
    2. With the increase in scanning speed both surface roughness and heat affected zone decreased for all values of laser power.
    3. With the increase in frequency HAZ and Ra decreased.
g) Regression analysis were done using the experimental results and predictive models were developed. ANOVA test was done to check the validity of the model.

h) Optimization using MOPSO was done to get optimum values of Power and scanning speed in order to fulfil the objective of getting maximum surface roughness and minimum heat affected zone. The optimum values of Power and Scanning speed obtained in case of Aluminium were 35W and 8mm/s and in case of Copper the values obtained were 15W and 4mm/s respectively.

6.2. Future Scope of The Work

Laser marking of light metal and alloys have tremendous potential for industrial applications. As such there are a number of areas in which further investigation of the present work can be carried out. Some of it has been mentioned below.

a) Since it was observed that while laser marking using Diode Pump Fiber Laser machine at the particular parameter settings led to formation of quite a thick re-solidified material at the top and the bottom edges of all the squares marked, investigation can be done on how to completely remove those accumulated material having burned edges.
b) The optimum values obtained can be utilised in some practical applications of laser marking for e.g. experiments on laser marking QR code and further improvement on the research can be accomplished if required.
c) Experimental investigation on Aluminium alloys like Al2024, Al50, etc. can be carried out since these materials hold great importance in the aviation and other industries that demand high strength to weight ratio materials for its applications.

REFERENCES

[1] Schaeffer, R. (2012). Fundamentals of laser micromachining. CRC press.

[2] Faisal, N., Zindani, D., Kumar, K., & Bhowmik, S. (2019). Laser micromachining of engineering materials—a review. Micro and Nano Machining of Engineering Materials, 121-136.

[3] Polmear, I., StJohn, D., Nie, J. F., & Qian, M. (2017). Light alloys: metallurgy of the light metals. Butterworth-Heinemann.

[4] Williams, E. (Ed.). (2016). *Light Metals 2016*. Springer.

[5] Carrilero, M. S., & Marcos, M. (1996). On the machinability of aluminium and aluminium alloys. *Journal of the Mechanical Behavior of Materials*, *7*(3), 179-194.

[6] Nagel, N. (2018). Beryllium and Copper-Beryllium Alloys. *ChemBioEng Reviews*, *5*(1), 30-33.

[7] Burgess, A., & Feng, K. (1998, November). Placing laser marking technology into production: The benefits of a new design tool. In International Congress on Applications of Lasers & Electro-Optics (Vol. 1998, No. 1, pp. D130-D139). Laser Institute of America.

[8] Chryssolouris, G. (2013). *Laser machining: theory and practice*. Springer Science & Business Media.

[9]Josefa, M., & Gándara, F. (2013). Aluminium: The Metal of Choice Aluminium: Kovina Izbire. *Mater. Technol.*, *3*(47), 261-265.

[10] Lazov, L., Deneva, H., & Narica, P. (2015, June). Laser marking methods. In *ENVIRONMENT. TECHNOLOGIES. RESOURCES. Proceedings of the International Scientific and Practical Conference* (Vol. 1, pp. 108-115).

[11] Lazov, L., Teirumnieks, E., Angelov, N., & Teirumnieka, E. (2019, June). Methodology for automatic determination of contrast of laser marking for different materials. In *ENVIRONMENT. TECHNOLOGIES. RESOURCES. Proceedings of the International Scientific and Practical Conference* (Vol. 3, pp. 134-136).

[12] Caiazzo, F., & Alfieri, V. (2018). Simulation of laser heating of aluminum and model validation via two-color pyrometer and shape assessment. *Materials*, *11*(9), 1506.

[13] Tam, A. C., Leung, W. P., & Krajnovich, D. (1991). Excimer laser ablation of ferrites. *Journal of applied physics*, *69*(4), 2072-2075.

[14] Conde, J. C., Lusquiños, F., González, P., Leon, B., & Pérez-Amor, M. (2001). Temperature distribution in laser marking. *Journal of Laser Applications*, *13*(3), 105-110.

[15] Tunna, L., Kearns, A., O'neill, W., & Sutcliffe, C. J. (2001). Micromachining of copper using Nd: YAG laser radiation at 1064, 532, and 355 nm wavelengths. *Optics & Laser Technology*, *33*(3), 135-143.

[16] Araujo, D., Carpio, F. J., Mendez, D., Garcıa, A. J., Villar, M. P., Garcıa, R., ... & Rubio, L. (2003). Microstructural study of CO2 laser machined heat affected zone of 2024 aluminum alloy. *Applied surface science*, *208*, 210-217.

[17] Qi, J., Wang, K. L., & Zhu, Y. M. (2003). A study on the laser marking process of stainless steel. *Journal of Materials Processing Technology*, *139*(1-3), 273-276.

[18] Lazov, L., & Angelov, N. (2012). Influence of some technological parameters on the contrast of laser marking on the fly. *Laser Physics*, *22*(11), 1755-1758.

[19] Li, C. L. (2014). Study of effect of laser marking Data Matrix symbols on titanium alloy

sheets using Nd: YAG laser. In *Advanced Materials Research* (Vol. 941, pp. 2165-2168). Trans Tech Publications Ltd.

[20] Sobotova, L., & Demec, P. (2015). Laser marking of metal materials. *Modern Machinery Science Journal*, 808-812.

[21] Schille, J., Schneider, L., Lickschat, P., Loeschner, U., Ebert, R., & Exner, H. (2015). High-pulse repetition frequency ultrashort pulse laser processing of copper. *Journal of laser applications*, *27*(S2), S28007.

[22] Li, X. S., He, W. P., Lei, L., Wang, J., Guo, G. F., Zhang, T. Y., & Yue, T. (2016). Laser direct marking applied to rasterizing miniature Data Matrix Code on aluminum alloy. *Optics & Laser Technology*, *77*, 31-39.

[23] Velotti, C., Astarita, A., Leone, C., Genna, S., Minutolo, F. M. C., & Squillace, A. (2016). Laser marking of titanium coating for aerospace applications. *Procedia Cirp*, *41*, 975-980.

[24] Švantner, M., Kučera, M., Smazalová, E., Houdková, Š., & Čerstvý, R. (2016). Thermal effects of laser marking on microstructure and corrosion properties of stainless steel. *Applied Optics*, *55*(34), D35-D45.

[25] Li, J., Lu, C., Wang, A., Wu, Y., Ma, Z., Fang, X., & Tao, L. (2016). Experimental investigation and mathematical modelling of laser marking two-dimensional barcodes on surfaces of aluminium alloy. *Journal of Manufacturing Processes*, *21*, 141-152.

[26] Li, C. L., & Lu, C. H. (2017). Laser direct-part marking of data matrix barcodes on the surface of metal alloy material. In *Key Engineering Materials* (Vol. 744, pp. 244-248). Trans Tech Publications Ltd.

[27] Bahaudin, M. Z., Bidin, N., & Bakhtiar, H. (2017). Laser surface roughening on copper analyzed using SEM-EDX. *Malaysian Journal of Fundamental and Applied Sciences*, *13*(4), 705-707.

[28] Mandal, K. K., Kuar, A. S., & Mitra, S. (2018). Experimental investigation on laser micro-machining of Al 7075 Alloy. *Optics & Laser Technology*, *107*, 260-267.

[29] Fraser, A., Maltais, J., & Godmaire, X. P. (2018, March). Analysis of laser marking performance on various non-ferrous metals. In *TMS Annual Meeting & Exhibition* (pp. 937-941). Springer, Cham.

[30] Naumova, M. G., Morozova, I. G., Zarapin, A. Y., & Borisov, P. V. (2018). Copper alloy marking by altering its surface topology using laser heat treatment. *Metallurgist*, *62*(5), 464-469.

[31] Kučera, M., Martan, J., & Franc, A. (2018). Time-resolved temperature measurement during laser marking of stainless steel. *International Journal of Heat and Mass Transfer*, *125*, 1061-1068.

[32] Leone, C., Bassoli, E., Genna, S., & Gatto, A. (2018). Experimental investigation and optimisation of laser direct part marking of Inconel 718. *Optics and Lasers in Engineering*, *111*, 154-166.

[33] Roy, A., Kumar, N., Das, S., & Bandyopadhyay, A. (2018). Optimization of Pulsed Nd: YVO4 Laser Marking of AISI 304 Stainless Steel Using Response Surface Methodology. *Materials Today: Proceedings*, *5*(2), 5244-5253.

[34] Shivakoti, I., Kibria, G., & Pradhan, B. B. (2019). Predictive model and parametric analysis of laser marking process on gallium nitride material using diode pumped Nd: YAG laser. *Optics & Laser Technology*, *115*, 58-70.

[35] Murzin, S. P., Liedl, G., & Pospichal, R. (2019). Coloration of a copper surface by nanostructuring with femtosecond laser pulses. *Optics & Laser Technology*, *119*, 105574.

[36] Li, X., Yang, L., Chang, B., Li, T., Li, C., Zhang, D., & Yan, B. (2020). Simulation and process optimization for laser marking of sub- millimeter rasterizing 2D code on stainless steel. *International Journal of Modern Physics B*, *34*(28), 2050266.

[37] Pavels, N., & Janis, F. (2020). Laser marking on plastic surfaces with minimal changes in material structure and maximum contrast. *Innovations*, *8*(2), 85-88.

[38] Sun, X., Wang, W., Mei, X., Pan, A., Zhang, J., & Li, G. (2020). Femtosecond laser dot-matrix marking on nickel-based alloy using a simple diaphragm-based spatial shaped modulation: Size and position control of marking units with high recognition rate. *Journal of Alloys and Compounds*, *835*, 155288.

[39] Du, Y., Zhang, L., Shu, T., Li, G., Chen, Y., Yang, W., & Zhang, X. (2021, August). Study the effect of single pulse energy on surface roughness of Aluminium alloy by laser marking. In *Sixteenth National Conference on Laser Technology and Optoelectronics* (Vol. 11907, p. 119070Y). International Society for Optics and Photonics.

[40] Atanasov, A., & Lengerov, A. (2021, June). Increasing the Effeciency of Laser Marking Ofaluminum Alloys by Double Writing of the Symbols. In *ENVIRONMENT. TECHNOLOGIES. RESOURCES. Proceedings of the International Scientific and Practical Conference* (Vol. 3, pp. 20-24).

[41]Lazov, L., Teirumnieks, E., Karadzhov, T., & Angelov, N. (2021). Influence of power density and frequency of the process of laser marking of steel products. *Infrared Physics & Technology*, *116*, 103783.

[42] Bravo-Montero, F., Castells-Rufas, D., & Carrabina, J. (2022). High-speed laser marking with diode arrays. *Optics & Laser Technology*, *146*, 107551

[43] Hamadi, H., Amara, E. H., Lavisse, L., Jouvard, J. M., Cicala, E., & Kellou, A. H. (2014). Contribution to laser marking parameters optimization.

[44] Conde, J. C., Paz, M. D., Serra, J., & González, P. (2014). Numerical and experimental study of the Ti6Al4V macrostructure obtained by Nd: YAG laser. *Applied Physics B*, *115*(1), 137-141.

[45] Venter, G. (2010). Review of optimization techniques.

[46] Wang, D., Tan, D., & Liu, L. (2018). Particle swarm optimization algorithm: an overview. Soft computing, 22(2), 387-408.

[47] Cui, Y., Meng, X., & Qiao, J. (2022). A multi-objective particle swarm optimization algorithm based on two-archive mechanism. *Applied Soft Computing*, *119*, 108532.

[48] Fraser, A., Brochu, V., Gingras, D., & Godmaire, X. P. (2016). Important considerations for laser marking an identifier on aluminum. In *Light Metals 2016* (pp. 261-264). Springer, Cham.

[49] Eberhart, R., & Kennedy, J. (1995, October). A new optimizer using particle swarm theory. In *MHS'95. Proceedings of the sixth international symposium on micro machine and human science* (pp. 39-43). Ieee.